Journal of Solid State Chemistry 181 (2008) 1258–1272

Contents lists available at ScienceDirect

Journal of Solid State Chemistry

journal homepage: www.elsevier.com/locate/jssc

Crystal chemistry of the divalent cation in alluaudite-type phosphates: A structural and infrared spectral study of the $Na_{1.5}(Mn_{1-x}M_x^{2+})_{1.5}Fe_{1.5}(PO_4)_3$ solid solutions ($x = 0$ to 1, $M^{2+} = Cd^{2+}$, Zn^{2+})

Frédéric Hatert *

Laboratoire de Minéralogie, Université de Liège, Bâtiment B18, B-4000 Liège, Belgium

ARTICLE INFO

Article history:
Received 30 May 2007
Received in revised form
22 February 2008
Accepted 27 February 2008
Available online 5 March 2008

Keywords:
Crystal chemistry
Divalent cation
Alluaudite structure
Na–Mn–Fe-phosphate

ABSTRACT

Compounds of the $Na_{1.5}(Mn_{1-x}M_x^{2+})_{1.5}Fe_{1.5}(PO_4)_3$ ($M^{2+} = Cd^{2+}$, Zn^{2+}) alluaudite-type solid solutions were synthesized by solid-state reactions in air, between 800 and 900 °C, and were investigated by X-ray powder diffraction and infrared spectroscopy. The site occupancy factors of the $Na_{1.5}(Mn_{1-x}Cd_x^{2+})_{1.5}Fe_{1.5}(PO_4)_3$ compounds, obtained from the Rietveld refinements of the X-ray powder patterns, indicate that the replacement of Mn^{2+} by Cd^{2+} takes place on the $M(1)$ site for $x = 0.25$ and 0.50, and then on the $M(1)$ and $M(2)$ sites for $x = 0.75$ and 1.00. Small amounts of Cd^{2+} were also detected on the $A(1)$ site, compensated by small amounts of Na^+ occurring on $M(1)$. This partially disordered distribution is probably due to the similar effective ionic radii of Cd^{2+} and Na^+. The cationic distributions in the $Na_{1.5}(Mn_{1-x}Zn_x^{2+})_{1.5}Fe_{1.5}(PO_4)_3$ solid solution indicate that Zn^{2+} was first introduced in the $M(2)$ site, before to replace Mn^{2+} in the $M(1)$ site. The unit-cell parameters show a significant increase when Mn^{2+} is replaced by Cd^{2+}, and a significant decrease when it is replaced by Zn^{2+}. The variations of the β angle were also correlated with the $M(1)$–$M(2)$ distances. The infrared spectra show the displacement of an absorption band at ca. 400–425 cm^{-1}, which is assigned to the vibrations of the M^{2+} cations localized on the $M(1)$ site. This assignment is confirmed by the excellent correlations between the $M(1)$–O bond distances and the energy of the absorption band.

1. Introduction

The alluaudite mineral group consists of Na–Mn–Fe-bearing phosphates, which occur in granitic pegmatites, particularly in the beryl-columbite-phosphate subtype of the rare-element pegmatites [1]. The crystal structure of alluaudite (monoclinic $C2/c$, $Z = 4$) consists of kinked chains of edge-sharing octahedra stacked parallel to {101} [2]. These chains are formed by a succession of $M(2)$ octahedral pairs linked by highly distorted $M(1)$ octahedra. Equivalent chains are connected in the b direction by the P(1) and P(2) phosphate tetrahedra to form sheets oriented perpendicular to [010]. These interconnected sheets produce channels parallel to c, that contain the distorted cubic $A(1)$ site and the $A(2)'$ site which exhibits a morphology of gable disphenoid. The general structural formula of alluaudite-type phosphates is $[A(2)A(2)']$ $[A(1)A(1)'A(1)''_2]M(1)M(2)_2(PO_4)_3$ [3]; in natural alluaudites, the large crystallographic A sites are occupied by Na^+, Ca^{2+} or Mn^{2+}, and the distorted octahedral M sites are occupied by Mn^{2+}, Fe^{2+}, Fe^{3+}, Al^{3+} or Mg^{2+} [4].

Over the past 20 years, many synthetic alluaudite-type phosphates, arsenates and molybdates have been reported [3,5–9]. The replacement of Na^+ by Li^+ on the large $A(1)$ site was demonstrated by the structural study of the $(Na_{1-x}Li_x)MnFe_2(PO_4)_3$ [3], $(Na_{1-x}Li_x)CdIn_2(PO_4)_3$ [10], and $(Na_{1-x}Li_x)_{1.5}Mn_{1.5}Fe_{1.5}(PO_4)_3$ [5] solid solutions, whereas the role of the trivalent cation was investigated in the $NaMn(Fe_{1-x}In_x)_2(PO_4)_3$ solid solution [11] and in the $Na_2Cd_2M^{3+}(PO_4)_3$ ($M^{3+} = In^{3+}$, Ga^{3+}, Cr^{3+}) compounds [12]. Extensive Mössbauer spectral studies [6,11,13–15] have shown the existence of next–nearest neighbor interactions affecting the iron atoms localized in the M sites.

The flexibility of the alluaudite structure will, no doubt, permit the use of alluaudite-type phosphates for practical applications, such as corrosion inhibition, passivation of metal surfaces, and catalysis [16,17]. Due to the presence of channels parallel to c-axis, alluaudite-type compounds exhibit electronic and/or ionic conductivity properties [18–20]. The possibility of inserting variable amounts of lithium into the channels of the alluaudite structure also makes the $(Na_{1-x}Li_x)MnFe_2^{3+}(PO_4)_3$ and $(Na_{1-x}Li_x)_{1.5}Mn_{1.5}Fe_{1.5}^{3+}(PO_4)_3$ compounds of value as potential battery materials [3,5,21].

The crystal chemistry of the divalent cation in alluaudite-type arsenates has been widely investigated, and the syntheses of

* Fax: +32 4 366 22 02.
E-mail address: fhatert@ulg.ac.be

0022-4596/$ - see front matter © 2008 Elsevier Inc. All rights reserved.
doi:10.1016/j.jssc.2008.02.035

$AgCo_3^{2+}H_2(AsO_4)_3$, $AgZn_3^{2+}H_2(AsO_4)_3$ [22] and $AgCu_4^{2+}(AsO_4)_3$ [23] have shown the presence of Co^{2+}, Zn^{2+}, and Cu^{2+} in the $M(1)$ and $M(2)$ sites. In the compounds $M^+Ca_2Mg_2(AsO_4)_3$ ($M^+ = K^+$, Na^+) [24], Ca^{2+} and Mg^{2+} occur in $M(1)$ and $M(2)$, respectively, while both M sites are filled by Mn^{2+} in $M^+Mn_3(AsO_4)(HAsO_4)_2$ ($M^+ = K^+$, Na^+) [25]. In synthetic phosphates, the M sites can be filled by Fe^{2+} in $NaFe_{3.67}(PO_4)_3$ [16], by Mn^{2+} in $M^+Mn_3(PO_4)(HPO_4)_2$ ($M^+ = Ag^+$, Na^+) [26,27], or by Co^{2+} in $M^+Co_3(PO_4)(HPO_4)_2$ ($M^+ = Ag^+$, Na^+) [28,29]. Mg^{2+} occupies the $M(1)$ site in $Na_2Mg_2Fe(PO_4)_3$ [12] and the $M(2)$ site in $NaCaCdMg_2(PO_4)_3$ [30], while significant amounts of Cd^{2+} occur in both M sites of $Na_2Cd_2M^{3+}(PO_4)_3$ ($M^{3+} = In^{3+}$, Ga^{3+}, Cr^{3+}) [12].

Although the experimental studies on alluaudite-type phosphates lead to a better understanding of the crystallochemical roles of Fe^{2+}, Mn^{2+}, Co^{2+}, Mg^{2+}, and Cd^{2+}, the crystal chemistry of Zn^{2+}, Cu^{2+} and Ni^{2+} was never investigated in detail. Because Zn^{2+} plays a significant role in natural alluaudites, in which 0.23 wt% ZnO were reported [4], we decided to perform solid-state

Table 1
Experimental details for the Rietveld refinements of the $Na_{1.5}(Mn_{1-x}M_x^{2+})_{1.5}Fe_{1.5}^{3+}(PO_4)_3$ (M^{2+} = Cd, Zn) alluaudite-type phosphates

Run #	S.027	S.217	S.218	S.219	S.209	S.220	S.221	S.222	S.213
Number of reflections	504	504	506	509	509	504	500	493	488
Refined parameters	55	54	54	54	55	51	52	53	51
Atomic coordinates	27	27	27	27	27	27	27	27	27
Site occupancy factors	4	3	3	4	4	1	2	3	2
Temperature factors	6	6	6	5	6	5	5	5	4
Unit-cell parameters	4	4	4	4	4	4	4	4	4
Background	5	5	5	5	5	5	5	5	5
Reflections profile	5	5	5	5	5	5	5	5	5
Zero point (°2θ)	1	1	1	1	1	1	1	1	1
Sample displacement	1	1	1	1	1	1	1	1	1
Sample transparency	1	–	–	–	–	–	–	–	–
Scale factor	–	1	1	1	1	1	1	1	1
Preferred orientation	1	1	1	1	1	1	1	1	1
R_p (%)	1.74	1.96	2.10	2.57	3.25	2.24	2.41	2.72	3.51
R_{wp} (%)	2.35	2.52	2.75	3.45	4.25	3.06	3.24	3.72	4.76
$R_{exp.}$ (%)	1.37	1.67	1.90	2.19	2.45	1.45	1.52	1.62	1.78
S (GooF)	1.71	1.50	1.44	1.56	1.73	2.09	2.11	2.28	2.66
R_{Bragg} (%)	3.40	3.18	3.03	2.89	4.19	4.41	4.46	4.18	7.66
a (Å)*	12.018(2)	12.064(2)	12.132(2)	12.188(3)	12.234(2)	11.950(3)	11.883(2)	11.802(3)	11.737(1)
b (Å)*	12.591(2)	12.599(2)	12.620(2)	12.660(3)	12.696(2)	12.555(3)	12.530(2)	12.515(3)	12.503(2)
c (Å)*	6.442(1)	6.442(1)	6.451(2)	6.463(2)	6.475(1)	6.420(1)	6.412(1)	6.396(2)	6.386(1)
β (°)*	114.27(1)	114.31(1)	114.34(2)	114.41(2)	114.50(1)	114.07(2)	113.93(1)	113.70(2)	113.54(1)

* : The unit-cell parameters were calculated with the least-squares refinement program LCLSQ 8.4 [31], from the d-spacings calibrated with an internal standard of $Pb(NO_3)_2$.

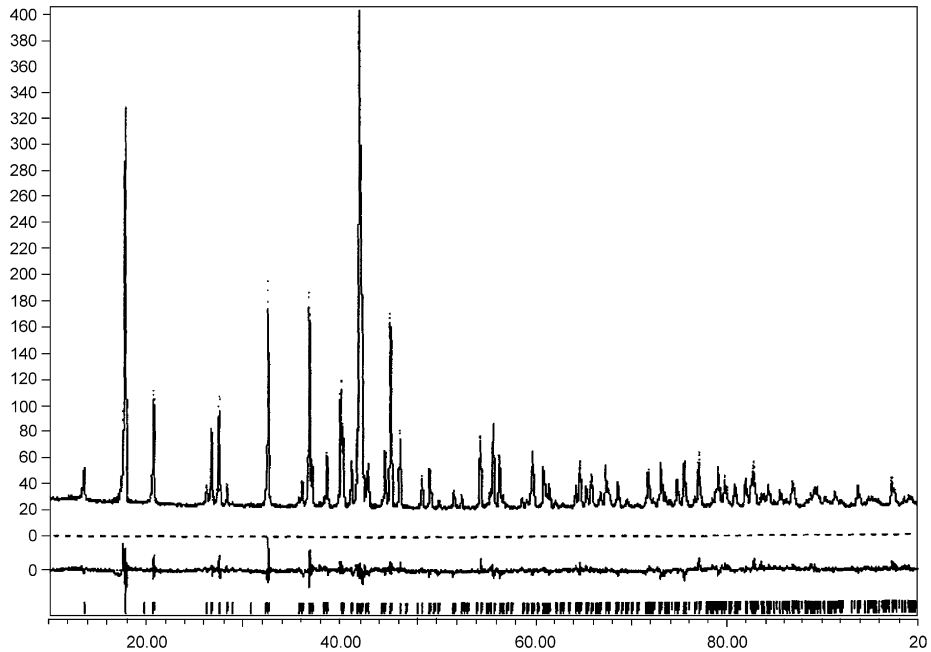

Fig. 1. The observed (dots), calculated (solid line) and difference X-ray powder diffraction patterns of $Na_{1.5}Zn_{1.5}Fe_{1.5}^{3+}(PO_4)_3$, obtained from a Rietveld refinement. The vertical markers indicate the calculated positions of the Fe$K\alpha_1$ and Fe$K\alpha_2$ Bragg reflections.

Table 2
Wet chemical analyses of the $Na_{1.5}(Mn_{1-x}M_x^{2+})_{1.5}Fe_{1.5}^{3+}(PO_4)_3$ (M^{2+} = Cd, Zn) alluaudite-type phosphates

	S.027	S.217	S.218	S.219	S.209	S.220	S.221	S.222	S.213
P_2O_5	43.96	41.04	40.08	38.41	37.10	42.97	42.53	42.47	42.39
Fe_2O_3*	24.14	23.33	22.98	22.26	19.59	25.02	24.75	20.03	16.79
FeO*	0.83	0.65	0.30	0.01	1.33	0.00	0.00	4.36	7.10
ZnO	–	–	–	–	–	6.26	12.20	20.9	28.1
MnO	21.10	14.60	9.35	4.31	0.00	15.10	9.80	4.63	0.00
CdO	-	10.28	18.98	26.32	35.51	–	–	–	–
Na_2O	9.42	8.32	8.15	7.92	7.50	8.70	8.64	8.58	8.45
Total	99.45	98.22	99.84	99.23	101.03	98.05	97.92	100.97	102.83
Cation numbers									
P	3.000	3.000	3.000	3.000	3.000	3.000	3.000	3.000	3.000
Fe^{3+*}	1.464	1.516	1.529	1.545	1.408	1.553	1.552	1.258	1.056
Fe^{2+*}	0.056	0.047	0.022	0.001	0.106	0.000	0.000	0.304	0.496
Zn	–	–	–	–	–	0.381	0.751	1.288	1.734
Mn	1.440	1.068	0.700	0.337	0.000	1.055	0.692	0.327	0.000
Cd	–	0.415	0.785	1.136	1.587	–	–	–	–
Na	1.472	1.393	1.397	1.417	1.389	1.391	1.396	1.388	1.370

Analyst : B. Belot. Cation numbers were calculated on the basis of 3 P per formula unit. *: the proportions of Fe_2O_3 and FeO were calculated to maintain charge balance.

Table 3
Results of synthesis experiments starting from the alluaudite-type compounds $NaMnFe_2^{3+}(PO_4)_3$ and $Na_{1.5}Mn_{1.5}Fe_{1.5}^{3+}(PO_4)_3$, in which the divalent cation has been progressively substituted

Solid solution	x	T (°C)	Synthesized compounds	Run #
$Na(Mn_{1-x}Ni_x)Fe_2^{3+}(PO_4)_3$	1.00	950	Alluaudite+α-$Na_7Fe_3(P_2O_7)_4$+$FePO_4$+?	S.199
$Na(Mn_{1-x}Mg_x)Fe_2^{3+}(PO_4)_3$	1.00	900	?	S.195
$Na(Mn_{1-x}Cu_x^{2+})Fe_2^{3+}(PO_4)_3$	1.00	900	$Cu_3Fe_4(PO_4)_6$+alluaudite+?	S.201
$Na(Mn_{1-x}Zn_x)Fe_2^{3+}(PO_4)_3$	1.00	900	Alluaudite+?	S.200
$Na(Mn_{1-x}Cd_x)Fe_2^{3+}(PO_4)_3$	0.25	900	Alluaudite+$FePO_4$	S.214
	0.50	900	Alluaudite+$FePO_4$	S.215
	0.75	900	Alluaudite+$FePO_4$	S.216
	1.00	800	Alluaudite+$FePO_4$	S.194
$Na(Mn_{1-x}Ca_x)Fe_2^{3+}(PO_4)_3$	1.00	950	?	S.003
$Na_{1.5}(Mn_{1-x}Ni_x)_{1.5}Fe_{1.5}^{3+}(PO_4)_3$	1.00	900	Alluaudite+α-$Na_7Fe_3(P_2O_7)_4$+?	S.210
$Na_{1.5}(Mn_{1-x}Mg_x)_{1.5}Fe_{1.5}^{3+}(PO_4)_3$	1.00	900	Alluaudite+?	S.211
$Na_{1.5}(Mn_{1-x}Cu_x^{2+})_{1.5}Fe_{1.5}^{3+}(PO_4)_3$	1.00	800	Alluaudite+$Cu_3(PO_4)_2$+?	S.212
$Na_{1.5}(Mn_{1-x}Zn_x)_{1.5}Fe_{1.5}^{3+}(PO_4)_3$	0.25	800	Alluaudite	S.220
	0.50	800	Alluaudite	S.221
	0.75	800	Alluaudite	S.222
	1.00	800	Alluaudite	S.213
$Na_{1.5}(Mn_{1-x}Cd_x)_{1.5}Fe_{1.5}^{3+}(PO_4)_3$	0.25	900	Alluaudite	S.217
	0.50	900	Alluaudite	S.218
	0.75	900	Alluaudite	S.219
	1.00	900	Alluaudite	S.209
$Na_{1.5}(Mn_{1-x}Ca_x)_{1.5}Fe_{1.5}^{3+}(PO_4)_3$	0.25	900	Alluaudite+? (tr.)	S.223
	0.50	900	Alluaudite+? (tr.)	S.224
	0.75	900	Alluaudite+? (tr.)	S.225
	1.00	900	Alluaudite+? (tr.)	S.208

Table 4
Atomic coordinates (x, y, z), isotropic temperature factors (B) and site occupancy parameters (N) for the $Na_{1.5}(Mn_{1-x}Cd_x)_{1.5}Fe_{1.5}^{3+}(PO_4)_3$ alluaudite-type phosphates

Site	Wyckoff	Atom	$Na_{1.5}Mn_{1.125}Cd_{0.375}Fe_{1.5}^{3+}(PO_4)_3$					$Na_{1.5}Mn_{0.75}Cd_{0.75}Fe_{1.5}^{3+}(PO_4)_3$				
			x	y	z	B(Å^2)	N	x	y	z	B(Å^2)	N
$A(2)'$	4*e*	Na	0	−0.0114(9)	1/4	0.3(4)	0.505(8)	0	−0.0133(9)	1/4	1.9(4)	0.553(8)
$A(1)$	4*b*	Na	1/2	0	0	1.8(2)	0.932(2)	1/2	0	0	1.5(2)	0.914(2)
		Cd	1/2	0	0	1.8(2)	0.068(2)	1/2	0	0	1.5(2)	0.086(2)
$M(1)$	4*e*	Mn	0	0.2666(2)	1/4	0.3(1)	0.630	0	0.2662(2)	1/4	0.5(1)	0.252
		Cd	0	0.2666(2)	1/4	0.3(1)	0.272(4)	0	0.2662(2)	1/4	0.5(1)	0.548(4)
		Na	0	0.2666(2)	1/4	0.3(1)	0.098(4)	0	0.2662(2)	1/4	0.5(1)	0.200(4)
$M(2)$	8*f*	Fe	0.2795(3)	0.6547(2)	0.3635(5)	0.8(1)	0.782	0.2779(2)	0.6543(1)	0.3632(4)	0.39(7)	0.776
		Mn	0.2795(3)	0.6547(2)	0.3635(5)	0.8(1)	0.219	0.2779(2)	0.6543(1)	0.3632(4)	0.39(7)	0.224
P(1)	4*e*	P	0	-0.2807(4)	1/4	0.6(1)	0.5	0	−0.2801(4)	1/4	0.98(9)	0.5
P(2)	8*f*	P	0.2395(3)	-0.1066(3)	0.1317(7)	0.6(1)	1.0	0.2406(3)	−0.1056(3)	0.1328(7)	0.98(9)	1.0
O(1)	8*f*	O	0.4530(6)	0.7121(5)	0.533(1)	0.5(1)	1.0	0.4518(6)	0.7106(5)	0.535(1)	0.91(8)	1.0
O(2)	8*f*	O	0.0982(6)	0.6401(5)	0.2379(9)	0.5(1)	1.0	0.0962(5)	0.6433(5)	0.2340(9)	0.91(8)	1.0
O(3)	8*f*	O	0.3295(6)	0.6621(5)	0.106(1)	0.5(1)	1.0	0.3252(6)	0.6606(5)	0.104(1)	0.91(8)	1.0

Table 4 (*continued*)

Site	Wyckoff	Atom	$Na_{1.5}Mn_{1.125}Cd_{0.375}Fe^{3+}_{1.5}(PO_4)_3$					$Na_{1.5}Mn_{0.75}Cd_{0.75}Fe^{3+}_{1.5}(PO_4)_3$				
			x	*y*	*z*	B(Å^2)	*N*	*x*	*y*	*z*	B(Å^2)	*N*
O(4)	8*f*	O	0.1292(6)	0.4036(5)	0.3222(9)	0.5(1)	1.0	0.1268(6)	0.4068(4)	0.3212(9)	0.91(8)	1.0
O(5)	8*f*	O	0.2278(6)	0.8252(5)	0.327(1)	0.5(1)	1.0	0.2314(6)	0.8263(5)	0.327(1)	0.91(8)	1.0
O(6)	8*f*	O	0.3204(4)	0.5024(7)	0.3815(8)	0.5(1)	1.0	0.3195(5)	0.5034(6)	0.3830(8)	0.91(8)	1.0
			$Na_{1.5}Mn_{0.375}Cd_{1.125}Fe^{3+}_{1.5}(PO_4)_3$					$Na_{1.5}Cd_{1.5}Fe^{3+}_{1.5}(PO_4)_3$				
A(2)′	4*e*	Na	0	−0.013(1)	1/4	1.0	0.541(6)	0	−0.014(1)	1/4	2.3(6)	0.56(1)
A(1)	4*b*	Na	1/2	0	0	1.4(2)	0.865(3)	1/2	0	0	1.2(2)	0.832(4)
		Cd	1/2	0	0	1.4(2)	0.136(3)	1/2	0	0	1.2(2)	0.168(4)
M(1)	4*e*	Cd	0	0.2665(2)	1/4	0.53(9)	0.773(7)	0	0.2666(2)	1/4	0.22(9)	0.792(8)
		Na	0	0.2665(2)	1/4	0.53(9)	0.227(7)	0	0.2666(2)	1/4	0.22(9)	0.208(8)
M(2)	8*f*	Fe	0.2764(2)	0.6533(1)	0.3608(4)	1.1(1)	0.773	0.2759(2)	0.6521(1)	0.3592(4)	1.04(9)	0.746(9)
		Mn	0.2764(2)	0.6533(1)	0.3608(4)	1.1(1)	0.104(7)	–	–	–	–	–
		Cd	0.2764(2)	0.6533(1)	0.3608(4)	1.1(1)	0.123(7)	0.2759(2)	0.6521(1)	0.3592(4)	1.04(9)	0.254(9)
P(1)	4*e*	P	0	−0.2789(5)	1/4	0.3(1)	0.5	0	−0.2778(5)	1/4	0.2(1)	0.5
P(2)	8*f*	P	0.2399(4)	−0.1047(3)	0.1335(7)	0.3(1)	1.0	0.2420(4)	−0.1033(3)	0.1347(8)	0.2(1)	1.0
O(1)	8*f*	O	0.4524(7)	0.7108(6)	0.535(1)	0.3(1)	1.0	0.4533(7)	0.7121(6)	0.540(1)	0.5(2)	1.0
O(2)	8*f*	O	0.0930(6)	0.6464(6)	0.232(1)	0.3(1)	1.0	0.0929(7)	0.6472(6)	0.229(1)	0.5(2)	1.0
O(3)	8*f*	O	0.3240(7)	0.6609(6)	0.098(1)	0.3(1)	1.0	0.3246(7)	0.6577(6)	0.094(1)	0.5(2)	1.0
O(4)	8*f*	O	0.1291(6)	0.4080(5)	0.324(1)	0.3(1)	1.0	0.1267(7)	0.4065(6)	0.324(1)	0.5(2)	1.0
O(5)	8*f*	O	0.2294(7)	0.8264(6)	0.325(1)	0.3(1)	1.0	0.2304(7)	0.8305(6)	0.319(2)	0.5(2)	1.0
O(6)	8*f*	O	0.3188(6)	0.5016(7)	0.382(1)	0.3(1)	1.0	0.3183(7)	0.4980(7)	0.376(1)	0.5(2)	1.0

Table 5
Atomic coordinates (*x*, *y*, *z*), isotropic temperature factors (*B*) and site occupancy parameters (*N*) for the $Na_{1.5}(Mn_{1-x}Zn_x)_{1.5}Fe^{3+}_{1.5}(PO_4)_3$ alluaudite-type phosphates

Site	Wyckoff	Atom	$Na_{1.5}Mn_{1.125}Zn_{0.375}Fe^{3+}_{1.5}(PO_4)_3$					$Na_{1.5}Mn_{0.75}Zn_{0.75}Fe^{3+}_{1.5}(PO_4)_3$				
			x	*y*	*z*	B(Å^2)	*N*	*x*	*y*	*z*	B(Å^2)	*N*
A(2)′	4*e*	Na	0	−0.007(1)	1/4	1.8(7)	0.49(1)	0	−0.008(1)	1/4	1.0	0.495(6)
A(1)	4*b*	Na	1/2	0	0	0.6(2)	1.00	1/2	0	0	0.6(2)	1.00
M(1)	4*e*	Mn	0	0.2658(3)	1/4	1.0	1.00	0	0.2670(3)	1/4	0.6(2)	0.76(2)
		Zn	–	–	–	–	–	0	0.2670(3)	1/4	0.6(2)	0.24(2)
M(2)	8*f*	Fe	0.2803(3)	0.6557(2)	0.3665(5)	1.36(9)	0.777	0.2807(3)	0.6543(2)	0.3668(5)	0.97(8)	0.776
		Mn	0.2803(3)	0.6557(2)	0.3665(5)	1.36(9)	0.032	–	–	–	–	–
		Zn	0.2803(3)	0.6557(2)	0.3665(5)	1.36(9)	0.191	0.2807(3)	0.6543(2)	0.3668(5)	0.97(8)	0.224
P(1)	4*e*	P	0	−0.2826(5)	1/4	0.2(1)	0.5	0	-0.2853(5)	1/4	0.4(1)	0.5
P(2)	8*f*	P	0.2405(4)	−0.1067(4)	0.1325(8)	0.2(1)	1.0	0.2385(4)	-0.1077(4)	0.1307(8)	0.4(1)	1.0
O(1)	8*f*	O	0.4599(7)	0.7130(6)	0.532(1)	0.3(1)	1.0	0.4566(7)	0.7142(6)	0.529(1)	0.3(1)	1.0
O(2)	8*f*	O	0.0975(8)	0.6375(5)	0.239(1)	0.3(1)	1.0	0.0999(8)	0.6382(5)	0.243(1)	0.3(1)	1.0
O(3)	8*f*	O	0.3269(7)	0.6636(6)	0.108(1)	0.3(1)	1.0	0.3253(7)	0.6637(6)	0.106(1)	0.3(1)	1.0
O(4)	8*f*	O	0.1267(7)	0.3989(6)	0.328(1)	0.3(1)	1.0	0.1269(7)	0.3983(5)	0.324(1)	0.3(1)	1.0
O(5)	8*f*	O	0.2270(6)	0.8246(6)	0.328(1)	0.3(1)	1.0	0.2263(6)	0.8272(6)	0.320(1)	0.3(1)	1.0
O(6)	8*f*	O	0.3202(6)	0.5020(8)	0.3808(9)	0.3(1)	1.0	0.3195(5)	0.5033(8)	0.3843(9)	0.3(1)	1.0
			$Na_{1.5}Mn_{0.375}Zn_{1.125}Fe^{3+}_{1.5}(PO_4)_3$					$Na_{1.5}Zn_{1.5}Fe^{3+}_{1.5}(PO_4)_3$				
A(2)′	4*e*	Na	0	−0.006(1)	1/4	1.0	0.484(6)	0	−0.004(1)	1/4	1.0	0.464(6)
A(1)	4*b*	Na	1/2	0	0	1.2(2)	0.992(9)	1/2	0	0	1.6(3)	0.98(1)
M(1)	4*e*	Mn	0	0.2671(2)	1/4	0.6(2)	0.46(2)	–	–	–	–	–
		Zn	0	0.2671(2)	1/4	0.6(2)	0.54(2)	0	0.2675(2)	1/4	2.0(1)	1.00
M(2)	8*f*	Fe	0.2828(2)	0.6539(2)	0.3697(5)	0.68(7)	0.781	0.2826(2)	0.6531(2)	0.3733(5)	0.62(7)	0.776
		Zn	0.2828(2)	0.6539(2)	0.3697(5)	0.68(7)	0.219	0.2826(2)	0.6531(2)	0.3733(5)	0.62(7)	0.224
P(1)	4*e*	P	0	−0.2872(4)	1/4	0.43(9)	0.5	0	−0.2919(5)	1/4	1.0	0.5
P(2)	8*f*	P	0.2392(4)	−0.1103(4)	0.1264(8)	0.43(9)	1.0	0.2345(4)	−0.1025(3)	0.1212(8)	1.0	1.0
O(1)	8*f*	O	0.4608(6)	0.7166(6)	0.538(1)	0.37(9)	1.0	0.4615(7)	0.7160(6)	0.543(1)	0.82(9)	1.0
O(2)	8*f*	O	0.1021(7)	0.6376(5)	0.243(1)	0.37(9)	1.0	0.1055(7)	0.6294(5)	0.247(1)	0.82(9)	1.0
O(3)	8*f*	O	0.3318(6)	0.6661(5)	0.115(1)	0.37(9)	1.0	0.3332(7)	0.6646(6)	0.095(1)	0.82(9)	1.0
O(4)	8*f*	O	0.1269(6)	0.3955(4)	0.328(1)	0.37(9)	1.0	0.1199(7)	0.3989(5)	0.312(1)	0.82(9)	1.0
O(5)	8*f*	O	0.2241(6)	0.8253(6)	0.323(1)	0.37(9)	1.0	0.2193(7)	0.8214(6)	0.310(2)	0.82(9)	1.0
O(6)	8*f*	O	0.3193(5)	0.5003(6)	0.3845(9)	0.37(9)	1.0	0.3232(5)	0.5067(7)	0.387(1)	0.82(9)	1.0

synthesis experiments, starting from the $Na(Mn_{1-x}M^{2+}_x)Fe_2(PO_4)_3$ and $Na_{1.5}(Mn_{1-x}M^{2+}_x)_{1.5}Fe_{1.5}(PO_4)_3$ (M^{2+} = Ni^{2+}, Mg^{2+}, Cu^{2+}, Zn^{2+},Cd^{2+}, Ca^{2+}) compositions. This paper gives the results of these experiments, and focuses particularly on the structural and infrared spectral characterization of the $Na_{1.5}(Mn_{1-x}M^{2+}_x)_{1.5}Fe_{1.5}(PO_4)_3$ (M^{2+} = Zn^{2+},Cd^{2+}) solid solutions.

2. Experimental

Compounds of the $Na(Mn_{1-x}M_x^{2+})Fe_2(PO_4)_3$ and $Na_{1.5}(Mn_{1-x}M_x^{2+})_{1.5}Fe_{1.5}(PO_4)_3$ ($M^{2+} = Ni^{2+}$, Mg^{2+}, Cu^{2+}, Zn^{2+},Cd^{2+}, Ca^{2+}) solid solutions were synthesized by solid-state reactions in air. Stoichiometric quantities of $NaHCO_3$ (Merck-Darmstadt, Germany—min. 99.5%), MnO (Alfa—Karlruhe, Germany—99.5%), NiO (Acros—Geel, Belgium—min. 99.5%) , MgO (UCB—Leuven, Belgium—min. 94.5%), CuO (UCB—min. 99%), ZnO (Merck—min. 99%), $CdCO_3$ (Acros—99.999%), $CaCO_3$ (Merck—min. 99%), $FeSO_4.7H_2O$ (Merck—min. 99.5%), and $NH_4H_2PO_4$ (Merck—min. 99%) were dissolved in concentrated nitric acid, and the resulting solution was evaporated to dryness. The dry residue was homogenized in an agate mortar, and then transferred into a platinum crucible where it was progressively heated at a final temperature of 800–950 °C. After 15–20 h, the experiment was ended by quenching the product in air.

The powder X-ray diffraction patterns of the compounds were recorded on a PHILIPS PW-3710 diffractometer using Fe$K\alpha$ radiation, with $\lambda = 1.9373$ Å. The unit-cell parameters of $Na_{1.5}(Mn_{1-x}M_x^{2+})_{1.5}Fe_{1.5}(PO_4)_3$ ($M^{2+} = Zn^{2+}$,Cd^{2+}) (Table 1) were calculated with the least-squares refinement program LCLSQ 8.4 [31], from the *d*-spacings calibrated with an internal standard of $Pb(NO_3)_2$. These unit-cell parameters and the atomic positions reported for $NaMnFe_2(PO_4)_3$ [3], served as starting parameters for the Rietveld refinements which were performed with the DBWS-9807 program [32]. The 2θ range extended from 10° to 100° with a step of 0.02° and a step time of 15 s. Experimental details for the Rietveld refinements are given in Table 1, and the final Rietveld plot for $Na_{1.5}Zn_{1.5}^{2+}Fe_{1.5}(PO_4)_3$ is shown in Fig. 1. Fits of equivalent quality were obtained for the other compounds.

The wet chemical analyses (Table 2) were performed using 65–102 mg of material. Na, Mn, Fe, Cd and Zn were determined with an Analytic Jena Novaa 300 atomic absorption spectrophotometer, whereas *P* was measured by colorimetry. The amounts of FeO and Fe_2O_3 were calculated to maintain charge balance.

Infrared spectra of $Na_{1.5}(Mn_{1-x}M_x^{2+})_{1.5}Fe_{1.5}(PO_4)_3$ ($M^{2+} = Zn^{2+}$,Cd^{2+}) were recorded with a Nicolet NEXUS spectrometer, from 32 scans with a 1 cm^{-1} resolution, over the 400–4000 cm^{-1}

Table 6
Selected interatomic distances (Å) and angles (°) for the $Na_{1.5}(Mn_{1-x}Cd_x)_{1.5}Fe_{1.5}^{3+}(PO_4)_3$ alluaudite-type phosphates

x	0.00	0.25	0.50	0.75	1.00	Difference
A(2)′–O(6) × 2	2.480(4)	2.472(4)	2.485(5)	2.492(6)	2.526(6)	0.05
A(2)′–O(6) × 2	2.643(3)	2.638(3)	2.671(4)	2.681(5)	2.671(6)	0.03
A(2)′–O(3) × 2	2.88(1)	2.88(1)	2.92(1)	2.94(1)	2.93(1)	0.05
A(2)′–O(1) × 2	2.84(1)	2.83(1)	2.79(1)	2.81(1)	2.80(1)	−0.04
Mean	2.71	2.71	2.72	2.73	2.73	0.02
A(1)–O(2) × 2	2.306(5)	2.318(6)	2.337(6)	2.359(7)	2.363(7)	0.06
A(1)–O(4) × 2	2.363(5)	2.356(6)	2.331(5)	2.344(6)	2.349(6)	−0.01
A(1)–O(4) × 2	2.567(4)	2.585(5)	2.566(5)	2.570(5)	2.564(6)	−0.00
A(1)–O(2) × 2	2.984(5)	3.003(6)	3.037(5)	3.057(6)	3.085(7)	0.10
Mean	2.56	2.57	2.57	2.58	2.59	0.03
M(1)–O(1) × 2	2.207(5)	2.228(6)	2.265(6)	2.259(6)	2.285(6)	0.08
M(1)–O(4) × 2	2.182(6)	2.242(6)	2.276(5)	2.300(6)	2.274(7)	0.09
M(1)–O(3) × 2	2.284(5)	2.293(6)	2.345(6)	2.368(7)	2.396(7)	0.11
Mean	2.22	2.25	2.30	2.31	2.32	0.10
M(2)-O(6)	1.984(8)	1.973(9)	1.976(8)	1.978(9)	2.015(9)	0.03
M(2)-O(3)	1.997(5)	1.988(6)	1.998(6)	2.012(6)	2.039(6)	0.04
M(2)-O(2)	1.985(5)	2.003(6)	2.025(4)	2.039(5)	2.040(6)	0.06
M(2)-O(5)	2.065(6)	2.053(6)	2.068(6)	2.077(6)	2.13(1)	0.07
M(2)-O(1)	2.081(5)	2.055(6)	2.079(5)	2.100(6)	2.134(6)	0.05
M(2)-O(5)	2.191(6)	2.225(7)	2.241(6)	2.254(8)	2.321(8)	0.13
Mean	2.05	2.05	2.06	2.08	2.11	0.06
M(1)–*M*(2)	3.331(2)	3.348(3)	3.379(2)	3.407(2)	3.426(2)	0.10
P(1)–O(1) × 2	1.547(7)	1.540(7)	1.519(7)	1.530(7)	1.492(7)	−0.06
P(1)–O(2) × 2	1.594(6)	1.575(6)	1.538(6)	1.517(7)	1.531(8)	−0.06
Mean	1.57	1.56	1.53	1.52	1.51	−0.06
P(2)-O(4)	1.536(4)	1.492(5)	1.508(5)	1.513(6)	1.520(7)	−0.02
P(2)-O(5)	1.574(6)	1.572(7)	1.551(7)	1.562(8)	1.51(1)	−0.06
P(2)-O(6)	1.512(8)	1.536(9)	1.522(8)	1.508(9)	1.470(9)	−0.04
P(2)-O(3)	1.560(7)	1.573(7)	1.553(7)	1.546(8)	1.527(8)	−0.03
Mean	1.55	1.54	1.53	1.53	1.51	−0.04
O(2)–P(1)–O(2)	101.4(4)	101.5(4)	103.1(4)	102.9(5)	103.1(5)	
O(1)–P(1)–O(2) × 2	107.8(3)	108.3(3)	108.0(3)	107.2(3)	106.5(3)	
O(1)–P(1)–O(2) × 2	115.1(3)	113.5(3)	113.8(3)	114.0(3)	114.3(3)	
O(1)–P(1)–O(1)	109.6(4)	111.6(5)	110.3(5)	111.5(5)	112.0(6)	
Mean	109.5	109.5	109.5	109.5	109.5	
O(4)-P(2)-O(3)	107.7(3)	108.9(3)	108.7(3)	107.3(4)	107.9(4)	
O(4)-P(2)-O(5)	107.0(3)	109.0(4)	109.2(4)	110.0(4)	110.2(4)	
O(5)-P(2)-O(6)	111.1(3)	109.7(3)	110.4(3)	111.0(4)	108.3(4)	
O(4)-P(2)-O(6)	112.6(3)	111.7(4)	110.8(3)	110.7(4)	114.2(5)	
O(6)-P(2)-O(3)	109.0(3)	107.1(4)	106.9(4)	108.1(4)	107.1(4)	
O(5)-P(2)-O(3)	109.4(4)	110.4(4)	110.8(4)	109.6(4)	109.1(5)	
Mean	109.5	109.5	109.5	109.5	109.5	

Estimated standard deviations on the mean values are smaller than 0.01 Å or than 0.5 °.

region. The samples were prepared by intimately mixing 2 mg of sample with KBr in order to obtain a 150 mg homogeneous pellet, which was subsequently dried for a few hours at 110 °C. To prevent water contamination, the measurements were performed under a dry air purge.

3. Results

3.1. Characterization of the compounds

The powder X-ray diffraction patterns of the synthesized phosphates show that the $Na_{1.5}(Mn_{1-x}M_x^{2+})_{1.5}Fe_{1.5}(PO_4)_3$ ($M^{2+} = Zn^{2+}$,Cd^{2+}) solid solutions are constituted by single-phase alluaudite-type compounds, whereas the Ni-, Cu-, Ca- and Mg-bearing phosphates contain supplementary phases which are sometimes undetermined (Table 3). The presence of these impurities forced us to focus our study on the $Na_{1.5}(Mn_{1-x}M_x^{2+})_{1.5}Fe_{1.5}(PO_4)_3$ ($M^{2+} = Zn^{2+}$,Cd^{2+}) compounds, which crystallize in fine-grained yellowish to greenish powders.

The wet chemical analyses of the $Na_{1.5}(Mn_{1-x}M_x^{2+})_{1.5}Fe_{1.5}(PO_4)_3$ ($M^{2+} = Zn^{2+}$,Cd^{2+}) compounds (Table 2) show chemical compositions fairly close to the starting compositions. The calculated Fe^{2+}-contents, which generally range between 0 and 7 atomic % Fe^{2+}, are in good agreement with the value of ca. 5% obtained by Mössbauer spectrometry for $Na_{1.5}Mn_{1.5}Fe_{1.5}^{3+}(PO_4)_3$ [5]. The two Zn-richest compounds, however, show a significant increase of the Fe^{2+}-content, which reaches 19–32 atomic % Fe^{2+}. This feature can be explained by the unexpected high Zn-contents of these synthetic compounds, compared to their ideal starting compositions. The Fe-contents, reaching ca. 1.55 atoms per formula unit (*a.p.f.u.*), are slightly higher than the nominal values, while the Mn- and Na-contents (ca. 1.4 *a.p.f.u.*) are significantly lower than these values.

3.2. Structure refinements

The positional parameters, site occupancies, isotropic temperature factors and interatomic distances and angles, deduced

Table 7
Selected interatomic distances (Å) and angles (°) for the $Na_{1.5}(Mn_{1-x}Zn_x)_{1.5}Fe_{1.5}^{3+}(PO_4)_3$ alluaudite-type phosphates.

x	0.00	0.25	0.50	0.75	1.00	Difference
A(2)′–O(6) × 2	2.480(4)	2.467(5)	2.455(5)	2.450(5)	2.420(5)	−0.06
A(2)′–O(6) × 2	2.643(3)	2.613(5)	2.620(4)	2.600(4)	2.562(4)	−0.08
A(2)′–O(3) × 2	2.88(1)	2.85(1)	2.87(1)	2.82(1)	2.74(1)	−0.14
A(2)′–O(1) × 2	2.84(1)	2.88(1)	2.88(1)	2.92(1)	2.96(1)	0.12
Mean	2.71	2.70	2.71	2.70	2.67	−0.04
A(1)–O(2) × 2	2.306(5)	2.308(6)	2.315(6)	2.311(6)	2.244(6)	−0.06
A(1)–O(4) × 2	2.363(5)	2.394(6)	2.391(6)	2.413(6)	2.311(6)	−0.05
A(1)–O(4) × 2	2.567(4)	2.540(6)	2.558(6)	2.544(5)	2.516(6)	−0.05
A(1)–O(2) × 2	2.984(5)	2.972(6)	2.952(6)	2.949(6)	2.898(6)	−0.09
Mean	2.56	2.55	2.55	2.55	2.49	−0.07
M(1)–O(1) × 2	2.207(5)	2.159(6)	2.154(6)	2.162(6)	2.168(6)	−0.04
M(1)–O(4) × 2	2.182(6)	2.184(8)	2.161(7)	2.113(5)	2.083(6)	−0.10
M(1)–O(3) × 2	2.284(5)	2.288(7)	2.284(7)	2.212(6)	2.174(7)	−0.11
Mean	2.22	2.21	2.20	2.16	2.14	−0.08
M(2)–O(6)	1.984(8)	1.95(1)	1.94(1)	1.960(8)	1.892(9)	−0.09
M(2)–O(3)	1.997(5)	1.940(6)	1.947(6)	1.941(6)	2.097(6)	0.10
M(2)–O(2)	1.985(5)	1.978(7)	1.969(7)	1.960(6)	1.950(6)	−0.04
M(2)–O(5)	2.065(6)	2.042(6)	2.055(6)	2.012(6)	2.02(1)	−0.05
M(2)–O(1)	2.081(5)	2.072(7)	2.055(7)	2.086(6)	2.097(6)	0.02
M(2)–O(5)	2.191(6)	2.198(8)	2.244(8)	2.237(8)	2.219(8)	0.03
Mean	2.05	2.03	2.04	2.03	2.05	0.00
M(1)–*M*(2)	3.331(2)	3.313(3)	3.303(3)	3.276(2)	3.271(2)	−0.06
P(1)–O(1) × 2	1.547(7)	1.577(7)	1.578(7)	1.532(7)	1.535(8)	−0.01
P(1)–O(2) × 2	1.594(6)	1.582(8)	1.552(8)	1.549(7)	1.595(7)	0.00
Mean	1.57	1.58	1.57	1.54	1.57	0.00
P(2)–O(4)	1.536(4)	1.513(6)	1.504(6)	1.494(5)	1.589(6)	0.05
P(2)–O(5)	1.574(6)	1.559(8)	1.516(8)	1.567(8)	1.63(1)	0.06
P(2)–O(6)	1.512(8)	1.55(1)	1.54(1)	1.541(8)	1.516(9)	0.00
P(2)–O(3)	1.560(7)	1.593(8)	1.576(8)	1.592(8)	1.531(8)	−0.03
Mean	1.55	1.55	1.53	1.55	1.57	0.02
O(2)–P(1)–O(2)	101.4(4)	101.2(5)	102.7(5)	104.8(4)	102.0(5)	
O(1)–P(1)–O(2) × 2	107.8(3)	107.1(3)	107.7(3)	106.9(3)	108.2(3)	
O(1)–P(1)–O(2) × 2	115.1(3)	115.3(3)	113.7(3)	114.4(3)	116.4(3)	
O(1)–P(1)–O(1)	109.6(4)	110.8(5)	111.3(5)	109.4(5)	106.1(5)	
Mean	109.5	109.5	109.5	109.5	109.6	
O(4)–P(2)–O(3)	107.7(3)	104.8(4)	105.2(4)	108.4(4)	112.9(4)	
O(4)–P(2)–O(5)	107.0(3)	109.3(4)	108.8(4)	108.8(4)	104.3(4)	
O(5)–P(2)–O(6)	111.1(3)	110.7(4)	110.8(4)	107.8(4)	110.8(4)	
O(4)–P(2)–O(6)	112.6(3)	112.7(5)	111.9(4)	112.7(4)	115.0(4)	
O(6)–P(2)–O(3)	109.0(3)	108.0(4)	108.3(4)	107.4(4)	110.7(4)	
O(5)–P(2)–O(3)	109.4(4)	111.2(4)	111.7(5)	111.7(4)	102.1(5)	
Mean	109.5	109.5	109.5	109.5	109.3	

Estimated standard deviations on the mean values are smaller than 0.01 Å or than 0.5 °.

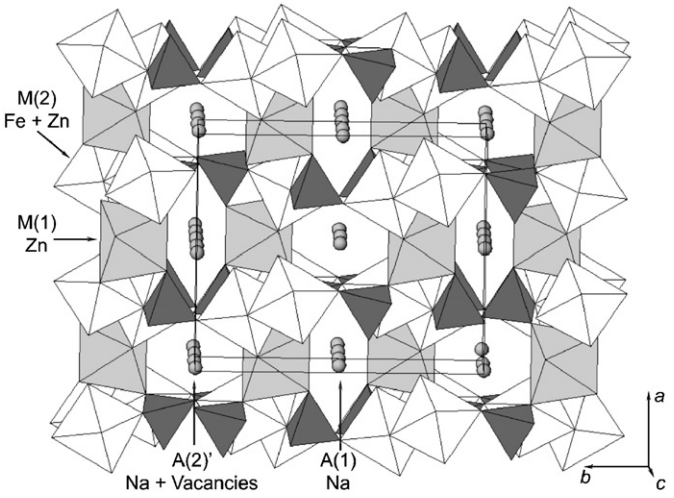

Fig. 2. Projection of the crystal structure of $Na_{1.5}Zn_{1.5}Fe^{3+}_{1.5}(PO_4)_3$. The PO_4 tetrahedra are densely shaded. The shaded $M(1)$ octahedra are occupied by Zn^{2+}, and the unshaded $M(2)$ octahedra are occupied by Fe and Zn^{2+}. The circles indicate Na^+ at the $A(1)$ and $A(2)'$ crystallographic sites.

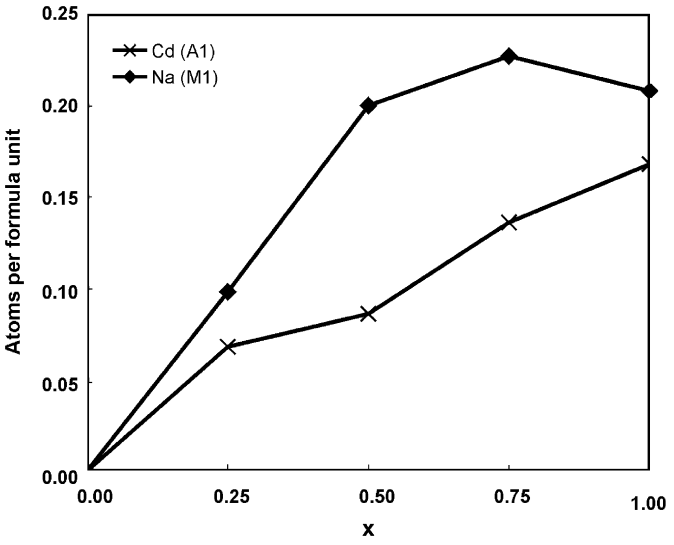

Fig. 3. Variations of the number of Cd^{2+} and Na^+ atoms occurring on the $A(1)$ and $M(1)$ crystallographic sites, in $Na_{1.5}(Mn^{2+}_{1-x}Cd_x)_{1.5}Fe^{3+}_{1.5}(PO_4)_3$.

from the Rietveld refinements of the powder X-ray diffraction patterns of the $Na_{1.5}(Mn_{1-x}M^{2+}_x)_{1.5}Fe_{1.5}(PO_4)_3$ ($M^{2+} = Zn^{2+}$,Cd^{2+}) alluaudite-type compounds ($x = 0.25$, 0.50, 0.75 and 1.00), are presented in Tables 4–7. The satisfactory R_p, R_{wp}, R_{Bragg}, and S values (Table 1), as well as the mean P–O distances and O–P–O angles (Tables 6 and 7), confirm the reliability of the refinements. A polyhedral representation of the crystal structure of $Na_{1.5}Zn^{2+}_{1.5}Fe_{1.5}(PO_4)_3$, approximately projected along [001], is shown in Fig. 2.

The positional parameters of the alluaudite-type compounds (Tables 4 and 5) correspond to the $A(2)'$, $A(1)$, $M(1)$ and $M(2)$ crystallographic sites, and the coordination polyhedra morphologies of $M(1)$ (very distorted octahedron), $M(2)$ (distorted octahedron), and $A(2)'$ (gable disphenoid), are similar to those previously described for many synthetic alluaudite-type phosphates [3,5,6,11,14,30]. The $A(1)$ site, however, shows a morphology of distorted cube in the $Na_{1.5}(Mn_{1-x}Zn^{2+}_x)_{1.5}Fe_{1.5}(PO_4)_3$ solid solution, and of distorted octahedron in the $Na_{1.5}(Mn_{1-x}Cd^{2+}_x)_{1.5}Fe_{1.5}(PO_4)_3$ solid solution, if we exclude the $A(1)$–O bond distances longer than 3.0 Å. The morphology of distorted cube is common

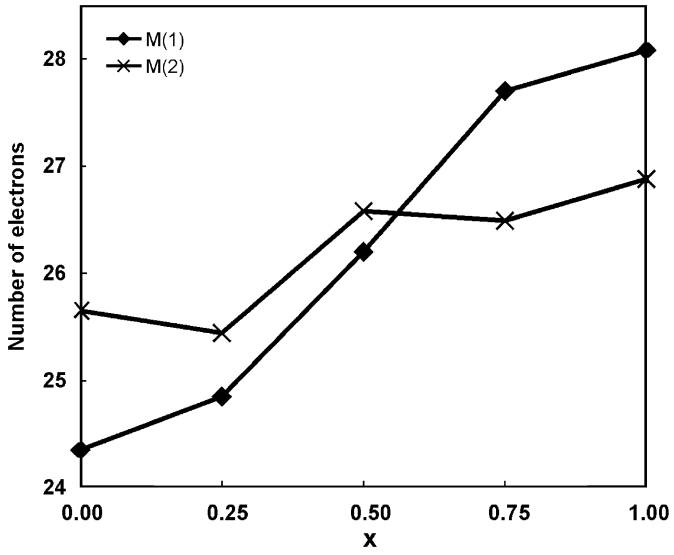

Fig. 4. Variations of the number of electrons occurring on the $M(1)$ and $M(2)$ crystallographic sites in $Na_{1.5}(Mn^{2+}_{1-x}Zn_x)_{1.5}Fe^{3+}_{1.5}(PO_4)_3$, obtained from a preliminary Rietveld refinement without any constraint on the site occupancies.

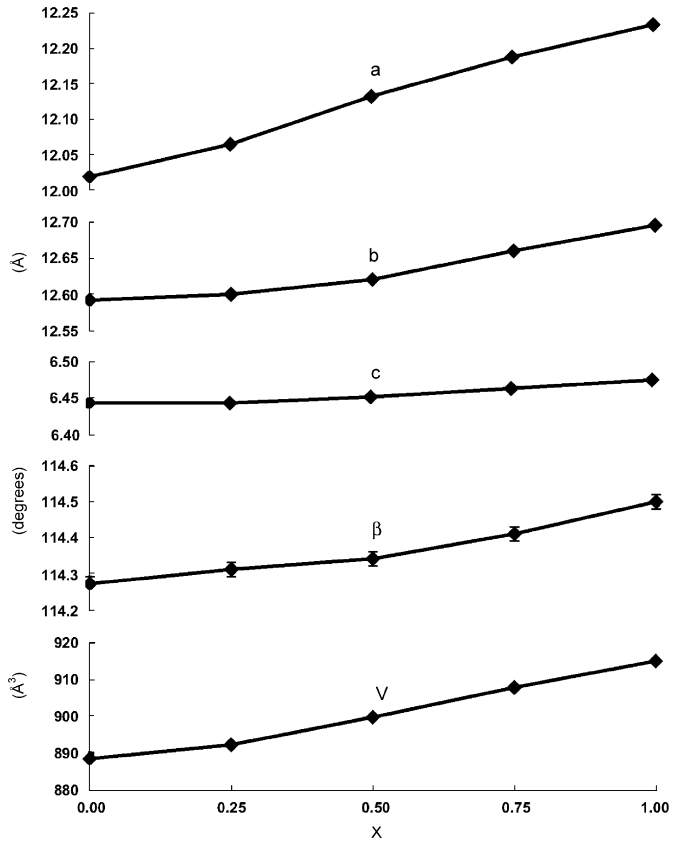

Fig. 5. The compositional dependence of the unit-cell parameters in $Na_{1.5}(Mn^{2+}_{1-x}Cd_x)_{1.5}Fe^{3+}_{1.5}(PO_4)_3$. The error bars are smaller than the data points.

for the $A(1)$ site of alluaudite-type compounds, but the morphology of distorted octahedron has only been observed in $(Na_{1-x}Li_x)CdIn_2(PO_4)_3$ [10,33].

The $M(1)$ and $M(2)$ site occupancy factors for $Na_{1.5}(Mn_{1-x}Cd^{2+}_x)_{1.5}Fe_{1.5}(PO_4)_3$ (Table 4) were constrained with the Fe- and Mn-contents obtained by the wet chemical analyses (Table 2). All iron was considered to be located in the $M(2)$ site,

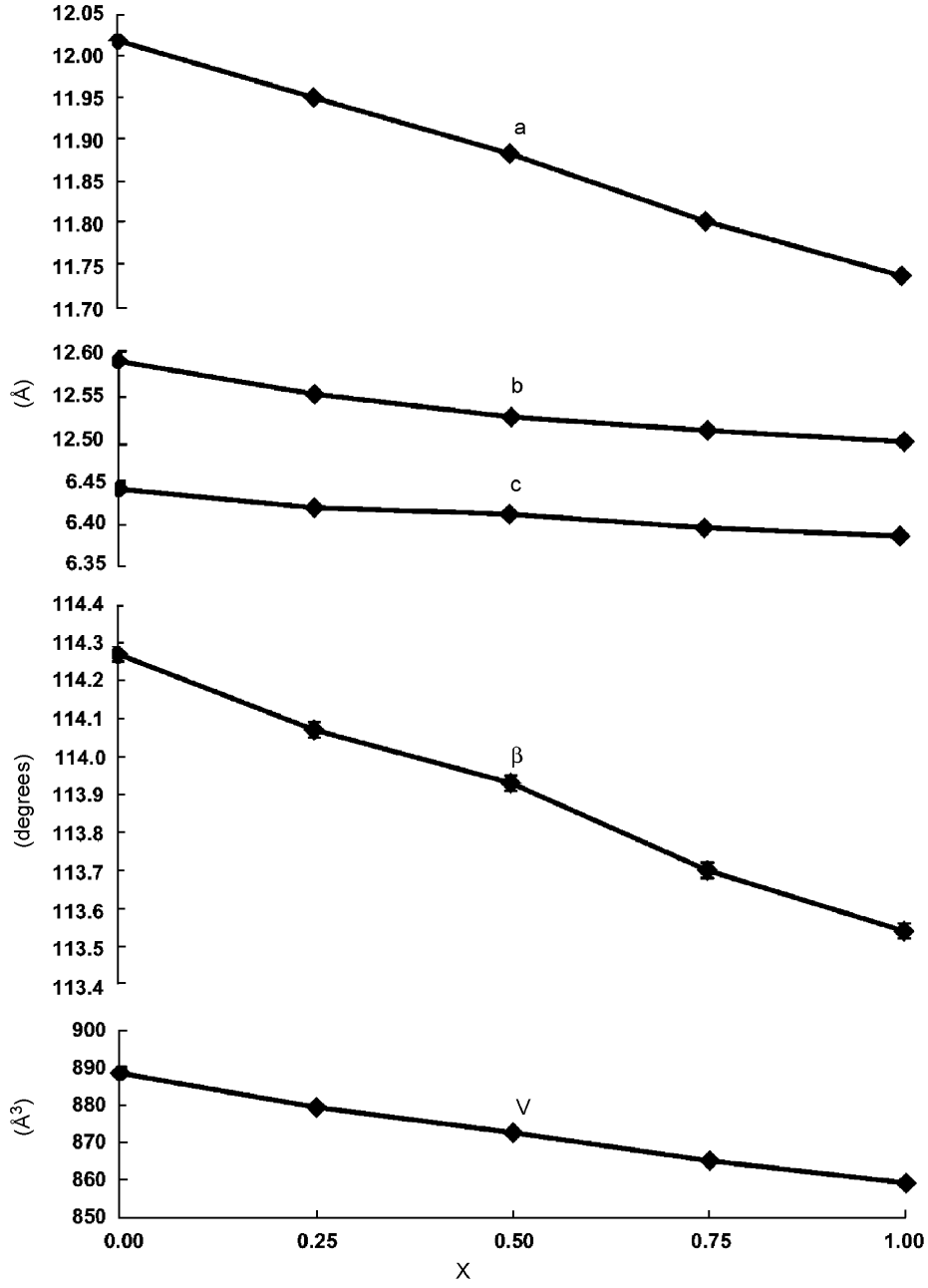

Fig. 6. The compositional dependence of the unit-cell parameters in $Na_{1.5}(Mn^{2+}_{1-x}Zn_x)_{1.5}Fe^{3+}_{1.5}(PO_4)_3$. The error bars are smaller than the data points.

and Mn was distributed over $M(2)$ and $M(1)$, according to the previous crystal-chemical investigations of alluaudite-type phosphates [2–6,10–15]. The number of electrons occurring in the M sites indicates that the replacement of Mn^{2+} by Cd^{2+} takes place on the $M(1)$ site for $x = 0.25$ and 0.50, and on the $M(1)$ and $M(2)$ sites for $x = 0.75$ and 1.00. Consequently, in the final model, Mn^{2+} (or Fe) against Cd^{2+} were refined on the $M(2)$ site ($x = 0.75$ and 1.00). These observations are in good agreement with the $M(1)$–O bond lengths, which show a significant increase between $x = 0.00$ and 0.50, whereas the $M(2)$–O bond lengths increase significantly between $x = 0.50$ and 1.00 (Table 6). The affinity of Cd^{2+} for the $M(1)$ site, clearly shown by these results, was previously demonstrated in the $NaCdIn_2(PO_4)_3$ and $NaCaCdMg_2(PO_4)_3$ alluaudite-type compounds [30,33].

In the preliminary refinement cycles, the electronic densities on $A(1)$ were unexpectedly high, while the electronic densities on $M(1)$ were lower than the expected values. These features indicate that small amounts of Cd^{2+} occur on the $A(1)$ site, compensated by small amounts of Na^+ on $M(1)$. In the final refinement cycle, Na^+ against Cd^{2+} were consequently refined on both $A(1)$ and $M(1)$ sites (Table 4). This partially disordered distribution is probably due to the similar effective ionic radii of Cd^{2+} and Na^+, which are 0.95 and 1.02 Å, respectively [34]. As shown in Fig. 3, the $M(1)$ site is able to accommodate a maximal amount of 0.23 Na^+ *a.p.f.u.*, an amount which is close to the 0.35 Na^+ *a.p.f.u.* observed in the $M(1)$ site of $Na_{1.70}Mn_{0.65}Fe^{3+}_2(PO_4)_3$. This last value probably corresponds to the maximal Na-content of the $M(1)$ site in alluaudite-type phosphates [35]. Fig. 3 also shows that the amount of Cd^{2+} occurring in the $A(1)$ site increases linearly when x increases, thus indicating that larger amounts of Cd^{2+} could be inserted in $A(1)$. This observation is in good agreement with the structural data obtained on $NaCaCdMg_2(PO_4)_3$, in which the $A(1)$ site is able to incorporate more that 50 mol% Cd^{2+} [30].

The cationic distributions in the $Na_{1.5}(Mn_{1-x}Zn_x^{2+})_{1.5}Fe_{1.5}(PO_4)_3$ compounds is more difficult to establish than for the Cd-bearing alluaudites, because the number of electrons of Zn^{2+} (28) is very close to the number of electrons of Fe^{3+} and Mn^{2+} (23). As shown in Fig. 4, however, the number of electrons detected on the $M(1)$ site increases significantly up to the value 28, thus indicating a complete replacement of Mn^{2+} by Zn^{2+} on this site. On the $M(2)$ site, the constant number of electrons between 0.50 and 1.00 shows that the introduction of Zn^{2+} took place between $x = 0.00$ and 0.50, an observation which demonstrates that Zn^{2+} was first introduced in the $M(2)$ site, before to replace Mn^{2+} in the $M(1)$ site (Table 5). In the final refinement cycle, the Fe- and Mn-contents of the $M(2)$ site were constrained with the values obtained by the wet chemical analyses (Table 2), whereas Mn^{2+} against Zn^{2+} were refined in the $M(1)$ site (Table 5).

A comparison of the nominal compositions of the $Na_{1.5}(Mn_{1-x}Cd_x^{2+})_{1.5}Fe_{1.5}(PO_4)_3$ and $Na_{1.5}(Mn_{1-x}Zn_x^{2+})_{1.5}Fe_{1.5}(PO_4)_3$ alluaudite-type compounds, with the compositions calculated from the site occupancy factors (Tables 4 and 5) and with those obtained by wet chemical analysis (Table 2), shows some discrepancies, especially for the $Na_{1.5}(Mn_{1-x}Cd_x^{2+})_{1.5}Fe_{1.5}(PO_4)_3$ solid solution. The Na-contents measured by chemical analysis (1.37–1.47 *a.p.f.u.*) are significantly lower than the nominal Na-content (1.5 *a.p.f.u.*), thus indicating that some volatile Na_2O was probably lost during the synthesis. The discrepancies observed between the chemical and structural data also illustrate the difficulty to infer accurate occupancies from Rietvled refinements, when many cations are taken into account.

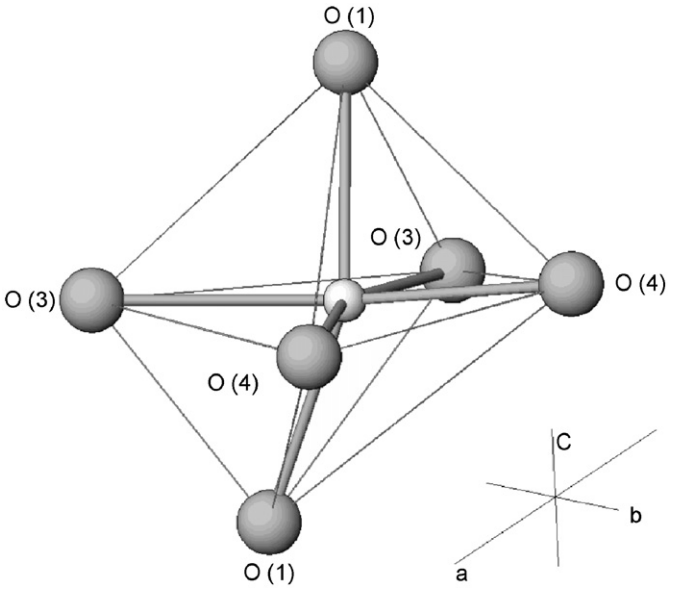

Fig. 7. Morphology of the $M(1)$ crystallographic site in $Na_{1.5}Mn_{0.75}^{2+}Cd_{0.75}Fe_{1.5}^{3+}(PO_4)_3$.

3.3. Variations of the unit-cell parameters

The unit-cell parameters of the $Na_{1.5}(Mn_{1-x}M_x^{2+})_{1.5}Fe_{1.5}(PO_4)_3$ ($M^{2+} = Zn^{2+}$,Cd^{2+}) alluaudite-type compounds (Table 1) show a significant increase when Mn^{2+} (effective ionic radius 0.830 Å, [29]) is replaced by Cd^{2+} (*e.i.r.* 0.95 Å) (Fig. 5), and a significant decrease when it is replaced by Zn^{2+} (*e.i.r.* 0.740) (Fig. 6).

These variations of unit-cell parameters can be correlated with the $M(1)$–O and $M(2)$O bond distances (Tables 6 and 7), which show significant variations in both solid solutions. In the $M(1)$ site, the bond distances most strongly affected by the Mn^{2+}–Cd^{2+} and Mn^{2+}–Zn^{2+} substitutions are $M(1)$–O(3) and $M(1)$–O(4) (Tables 6 and 7), which are forming a square approximately parallel to the *ab* plane (Fig. 7). These strong variations of bond distances are consequently responsible for the more pronounced variations of the *a* and *b* unit-cell parameters, compared to *c* (Figs. 5 and 6).

The variations of the β angle are also correlated with the $M(1)$–$M(2)$ distances, as shown in Figs. 8 and 9. Similar correlations were already observed in the $NaMn(Fe_{1-x}In_x)_2(PO_4)_3$ and $Na_2(Mn_{1-x}Fe_x^{2+})_2Fe^{3+}(PO_4)_3$ solid solutions [11,14], and can be qualitatively understood by a shortening or an elongation of the $M(1)$–$M(2)$ chains of the alluaudite structure, thus producing a decrease or an increase of the β angle, respectively (Fig. 10).

3.4. Infrared spectral results

The infrared spectra of the $Na_{1.5}(Mn_{1-x}Cd_x)_{1.5}Fe_{1.5}(PO_4)_3$ and $Na_{1.5}(Mn_{1-x}Zn_x)_{1.5}Fe_{1.5}(PO_4)_3$ solid solutions are shown in Figs. 11 and 12, respectively, and the assignment of their absorption bands (Table 8) was performed by comparison with those of the $NaMn(Fe_{1-x}In_x)_2(PO_4)_3$ and $Na_2(Mn_{1-x}Fe_x^{2+})_2Fe^{3+}(PO_4)_3$ alluaudite-type compounds [11,14]. According to the fundamental

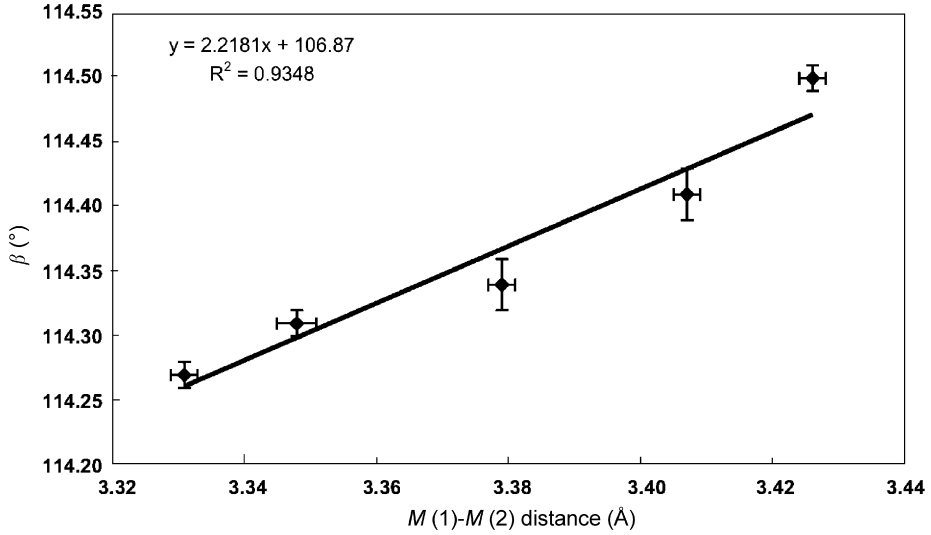

Fig. 8. Correlation between the β angle and the $M(1)$–$M(2)$ bond distance, in $Na_{1.5}(Mn_{1-x}^{2+}Cd_x)_{1.5}Fe_{1.5}^{3+}(PO_4)_3$.

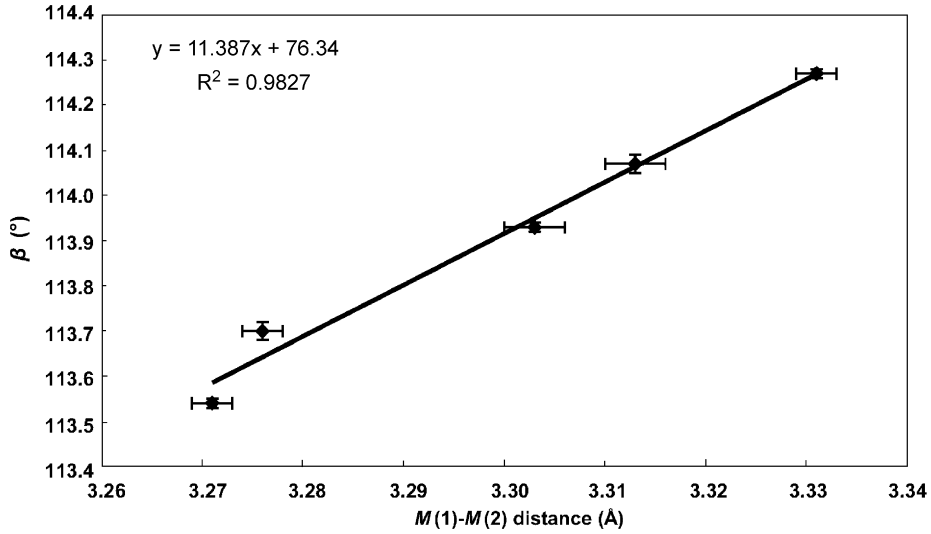

Fig. 9. Correlation between the β angle and the $M(1)$–$M(2)$ bond distance, in $Na_{1.5}(Mn^{2+}_{1-x}Zn_x)_{1.5}Fe^{3+}_{1.5}(PO_4)_3$.

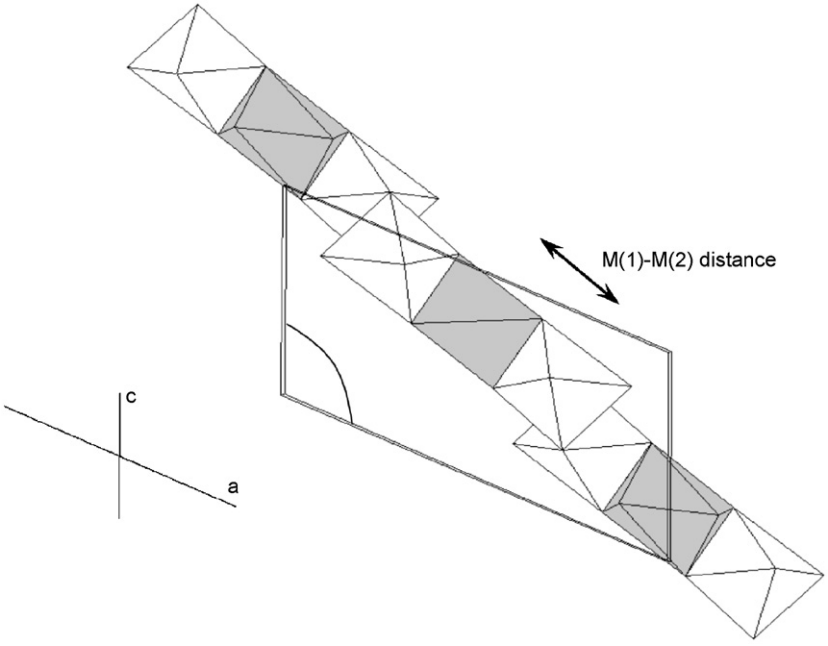

Fig. 10. Projection of the octahedral M chains of the alluaudite structure, showing the relationship between the $M(1)$–$M(2)$ distance and the β angle.

vibrational frequencies of the PO_4 tetrahedron [36], the absorption bands between 921 and 1103 cm^{-1} can be assigned to ν_3, the antisymmetric stretching modes of the PO_4 anions, and the bands between 518 and 594 cm^{-1} can be assigned to ν_4, their bending mode. The weak bands between 899 and 919 cm^{-1} probably correspond to ν_1, the symmetric stretching mode of the distorted PO_4 tetrahedron.

When Mn^{2+} is replaced by Cd^{2+} or Zn^{2+} in the $Na_{1.5}(Mn_{1-x}M^{2+}_x)_{1.5}Fe_{1.5}(PO_4)_3$ solid solutions, the infrared spectra show an important displacement of an absorption band found at 414 cm^{-1}, in the spectrum of $Na_{1.5}Mn_{1.5}Fe_{1.5}(PO_4)_3$ (Table 8). This band can be assigned to the vibrations of the M^{2+} cations localized on the $M(1)$ site, an assignment which is confirmed by the excellent correlations between the $M(1)$–O bond distances and the wavenumber of the absorption band (Figs. 13, 14). The replacement of Mn^{2+} by Cd^{2+} produces a lengthening of the $M(1)$–O bond lengths (Table 6), responsible for the decrease of the wavenumber from 414 to <400 cm^{-1}. On the contrary, the replacement of Mn^{2+} by Zn^{2+} produces a shortening of the $M(1)$–O bonds (Table 7), thus inducing an increase of the wavenumber from 414 to 426 cm^{-1} (Table 8). Similar displacements of the absorption band around 420 cm^{-1} were previously reported in the $Na_2(Mn_{1-x}M^{2+}_x)_2Fe^{3+}(PO_4)_3$ ($M^{2+} = Ca^{2+}$, Cd^{2+}, Ni^{2+}, Zn^{2+}, Mg^{2+}) compounds [37]. In the spectra of the $Na_{1.5}(Mn_{1-x}Cd^{2+}_x)_{1.5}Fe_{1.5}(PO_4)_3$ compounds, the absorption band at 466–471 cm^{-1} also shows a similar displacement, thus confirming its attribution to the vibrations of the M^{2+} cations localized on the $M(1)$ site.

4. Discussion

4.1. The role of the divalent cation in alluaudite-type phosphates

The results given in this paper show that in the $Na_{1.5}Mn_{1.5}Fe_{1.5}(PO_4)_3$ alluaudite-type phosphate, Mn^{2+} can be easily replaced by Zn^{2+} or by Cd^{2+}, whereas Ca^{2+}, Cu^{2+}, Mg^{2+} and Ni^{2+}

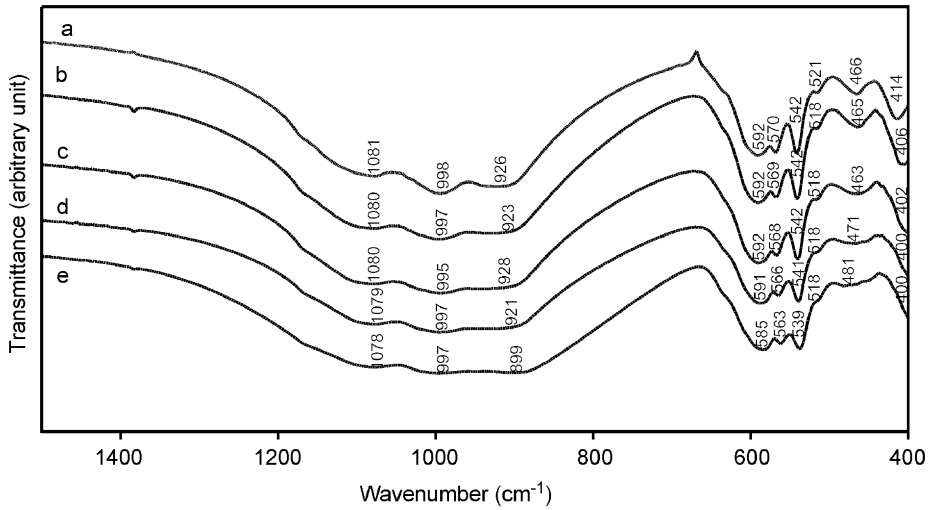

Fig. 11. Infrared spectra of the $Na_{1.5}(Mn^{2+}_{1-x}Cd_x)_{1.5}Fe^{3+}_{1.5}(PO_4)_3$ alluaudite-type compounds.

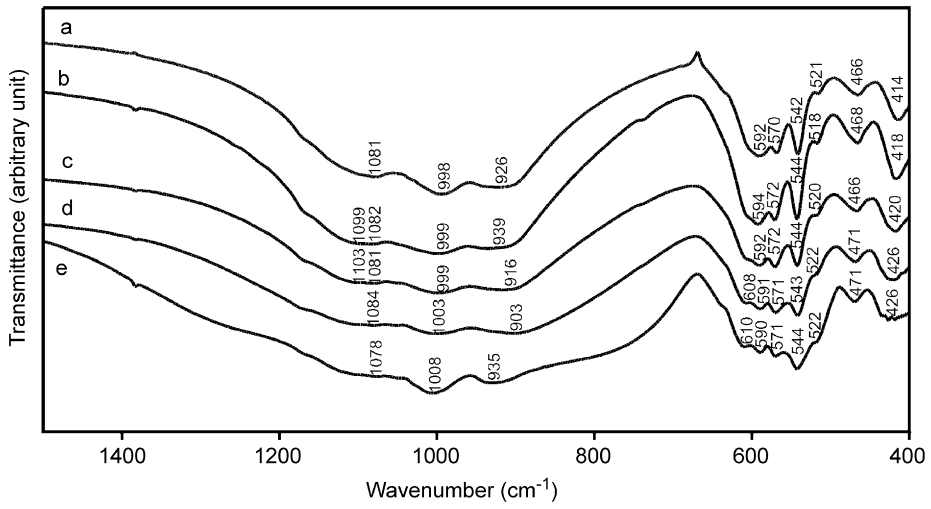

Fig. 12. Infrared spectra of the $Na_{1.5}(Mn^{2+}_{1-x}Zn_x)_{1.5}Fe^{3+}_{1.5}(PO_4)_3$ alluaudite-type compounds.

Table 8
Assignment of the infrared absorption bands for the $Na_{1.5}(Mn_{1-x}M^{2+}_x)_{1.5}Fe^{3+}_{1.5}(PO_4)_3$ (M^{2+} = Cd, Zn) alluaudite-type phosphates.

$x = 0$	0.25	0.50	0.75	1.00	Difference	Assignment
$Na_{1.5}(Mn_{1-x}Cd_x)_{1.5}Fe^{3+}_{1.5}(PO_4)_3$						
1081	1080	1080	1079	1078	−3	
998	997	995	997	997	−1	υ_3 PO_4
926	923	928	921	–	−5	
–	–	–	–	899		υ_1 PO_4
592	592	592	591	585	−7	
570	569	568	566	563	−7	υ_4 PO_4
542	542	542	541	539	−3	
521	518	518	518	518	−3	
466	465	463	–	–	−3	Mn^{2+}–$O_{M(2)}$
–	–	–	471	–		M^{2+}–$O_{M(2)}$
–	–	–	–	481		Cd–$O_{M(2)}$
414	406	402	400	< 400	> −14	M^{2+}–$O_{M(1)}$
$Na_{1.5}(Mn_{1-x}Zn_x)_{1.5}Fe^{3+}_{1.5}(PO_4)_3$						
–	1099	1103	–	–	4	
1081	1082	1081	1084	1078	−3	υ_3 PO_4
998	999	999	1003	1008	10	
926	939	–	–	935	9	
–	–	916	903	–	−13	υ_1 PO_4
–	604	606	608	610	6	M^{2+}–$O_{M(2)}$?
592	594	592	591	590	−2	
570	572	572	571	571	1	υ_4 PO_4
542	544	544	543	544	2	

Table 8 (*continued*)

$x = 0$	0.25	0.50	0.75	1.00	Difference	Assignment
521	518	520	522	522	1	υ_4 PO_4
466	468	466	471	471	5	M^{2+}–$O_{M(1)}$
414	418	420	426	426	12	M^{2+}–$O_{M(1)}$

Estimated standard deviations are ca. 1 cm^{-1}.

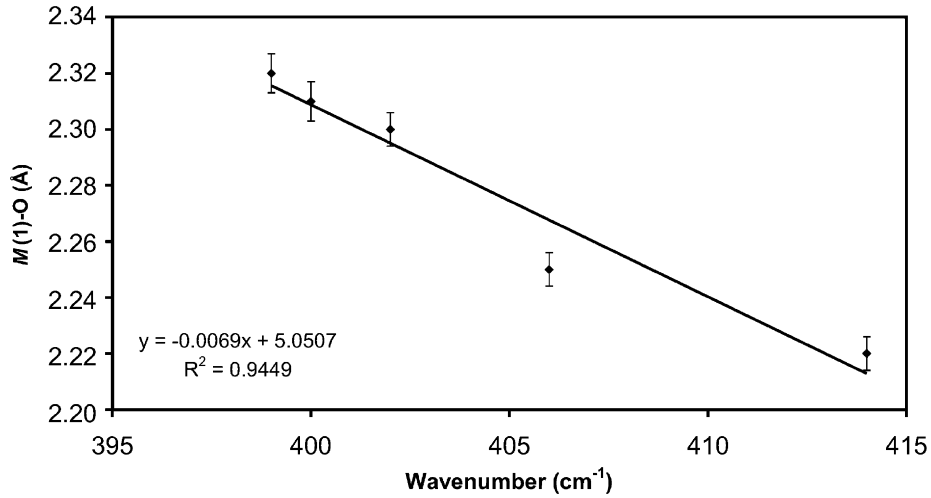

Fig. 13. Correlation between the $M(1)$–O distance and the wavenumber of the infrared absorption band located around 405 cm^{-1}, for the $Na_{1.5}(Mn^{2+}_{1-x}Cd_x)_{1.5}Fe^{3+}_{1.5}(PO_4)_3$ alluaudite-type compounds.

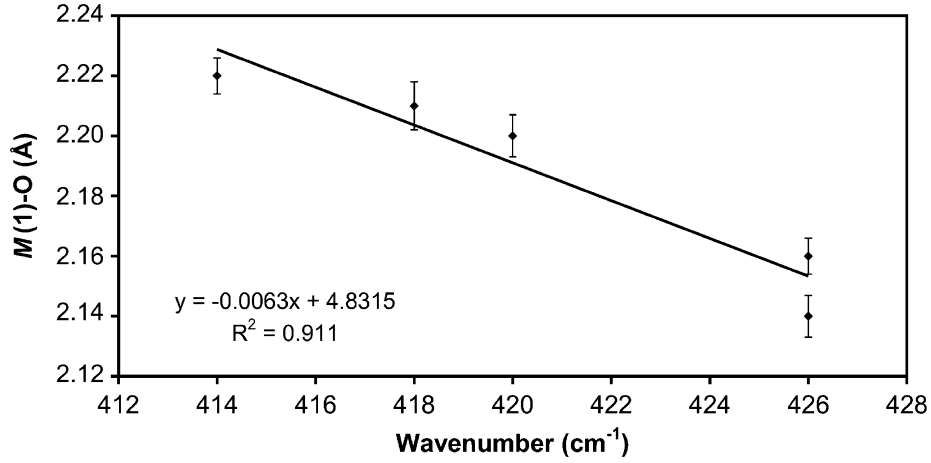

Fig. 14. Correlation between the $M(1)$–O distance and the wavenumber of the infrared absorption band located around 420 cm^{-1}, for the $Na_{1.5}(Mn^{2+}_{1-x}Zn_x)_{1.5}Fe^{3+}_{1.5}(PO_4)_3$ alluaudite-type compounds.

Table 9
Occupancy, effective ionic radii (*e.i.r.*, Å), and M–O distances (Å) for the $M(1)$ and $M(2)$ sites of alluaudite-type phosphates.

Compound	Occupancy $M(1)$	*e.i.r.* $M(1)$	$M(1)$-O (Å)	Occupancy $M(2)$	*e.i.r.* $M(2)$ (Å)	$M(2)$-O (Å)	References
$NaMnFe_2^{3+}(PO_4)_3$	0.95 Mn^{2+}+0.025 Mg+0.025 Li	0.826	2.206	0.99 Fe^{3+}+0.01 Mg	0.646	2.042	[2]
$Na_2Fe_2^{2+}Fe^{3+}(PO_4)_3$	Fe^{2+}	0.780	2.194	0.5 Fe^{2+}+0.5 Fe^{3+}	0.713	2.065	[51]
$Na_2Mg_2Fe^{3+}(PO_4)_3$	Mg	0.720	2.13	0.5 Mg+0.5 Fe^{3+}	0.683	2.04	[12]
$Na_2Cd_2Fe^{3+}(PO_4)_3$	0.79 Cd+0.21 Na	0.965	2.37	0.5 Cd+0.5 Fe^{3+}	0.798	2.13	[12]
$Na_2Cd_2Ga(PO_4)_3$	0.71 Cd+0.29 Na	0.970	2.36	0.5 Cd+0.5 Ga	0.785	2.13	[12]
$Na_2Cd_2Cr(PO_4)_3$	0.76 Cd+0.24 Na	0.967	2.36	0.5 Cd+0.5 Cr	0.783	2.09	[12]

Table 9 (*continued*)

Compound	Occupancy $M(1)$	*e.i.r.* $M(1)$	$M(1)$-O (Å)	Occupancy $M(2)$	*e.i.r.* $M(2)$ (Å)	$M(2)$-O (Å)	References
$NaCdIn_2(PO_4)_3$	Cd	0.950	2.30	In	0.800	2.14	[33]
$NaCo_3^{2+}(PO_4)(HPO_4)_2$	Co^{2+}	0.745	2.149	Co^{2+}	0.745	2.096	[29]
$NaCaCdMg_2(PO_4)_3$	0.42 Cd+0.58 Ca	0.979	2.31	Mg	0.720	2.09	[30]
$NaMn_3^{2+}(PO_4)(HPO_4)_2$	Mn^{2+}	0.830	2.236	Mn^{2+}	0.830	2.174	[26]
$AgMn_3^{2+}(PO_4)(HPO_4)_2$	Mn^{2+}	0.830	2.233	Mn^{2+}	0.830	2.178	[27]
$Na_3In_2(PO_4)_3$	Na	1.020	2.447	In	0.800	2.151	[45]
$NaFe_{3.67}(PO_4)_3$	Fe^{2+}	0.780	2.192	Fe^{2+}	0.780	2.085	[16]
$Ag_2Mn_2Fe^{3+}(PO_4)_3$	Mn^{2+}	0.830	2.242	0.5 Mn^{2+}+0.5 Fe^{3+}	0.738	2.093	[52]
$AgCo_3(PO_4)(HPO_4)_2$	Co^{2+}	0.745	2.243	Co^{2+}	0.745	2.093	[28]
$Na_2Mn_2Fe(PO_4)_3$	Mn^{2+}	0.830	2.248	0.5 Mn^{2+}+0.5 Fe^{3+}	0.738	2.117	[19]
$AgNaMn_2Fe(PO_4)_3$	Mn^{2+}	0.830	2.276	0.5 Mn^{2+}+0.5 Fe^{3+}	0.738	2.094	[19]
$AgNi_3(PO_4)(HPO_4)_2$	Ni	0.690	2.278	Ni	0.690	2.093	[53]
$Na_{1.79}Mg_{1.79}Fe_{1.21}(PO_4)_3$	Mg	0.720	2.286	0.605 Fe^{3+}+0.395 Mg	0.675	2.148	[54]
$Na_2CdMnFe(PO_4)_3$	Cd	0.950	2.286	0.5 Mn^{2+}+0.5 Fe^{3+}	0.738	2.095	[20]
$Na_4CaFe_4(PO_4)_6$	0.5 Ca+0.5 Na	1.010	2.323	Fe^{3+}	0.645	2.031	[55]
$NaMnFe_2^{3+}(PO_4)_3$	Mn^{2+}	0.830	2.204	Fe^{3+}	0.645	2.046	[3]
$Na_{1.5}Mn_{1.5}Fe_{1.5}^{3+}(PO_4)_3$	Mn^{2+}	0.830	2.22	0.75 Fe^{3+}+0.25 Mn^{2+}	0.691	2.05	[5]
$Na_2Mn_2Fe^{3+}(PO_4)_3$	0.92 Mn^{2+}+0.08 Na	0.846	2.31	0.5 Fe^{3+}+0.5 Mn^{2+}	0.738	2.10	[15]
$Mn_{2.25}Fe_{1.5}^{3+}(PO_4)_3$	Mn^{2+}	0.830	2.25	0.75 Fe^{3+}+0.25 Mn^{2+}	0.691	2.04	[35]
$Na_{0.5}Li_{0.5}MnFe_2^{3+}(PO_4)_3$	Mn^{2+}	0.830	2.201	Fe^{3+}	0.645	2.038	[3]
$NaCdIn_2(PO_4)_3$	Cd	0.950	2.33	In	0.800	2.14	[10]
$Na_{0.75}Li_{0.25}CdIn_2(PO_4)_3$	Cd	0.950	2.34	In	0.800	2.14	[10]
$Na_{0.5}Li_{0.5}CdIn_2(PO_4)_3$	Cd	0.950	2.33	In	0.800	2.15	[10]
$Na_{1.125}Li_{0.375}Mn_{1.5}Fe_{1.5}^{3+}(PO_4)_3$	Mn^{2+}	0.830	2.25	0.75 Fe^{3+}+0.25 Mn^{2+}	0.691	2.05	[5]
$Na_{0.75}Li_{0.75}Mn_{1.5}Fe_{1.5}^{3+}(PO_4)_3$	Mn^{2+}	0.830	2.24	0.75 Fe^{3+}+0.25 Mn^{2+}	0.691	2.05	[5]
$NaMnFe_{1.5}^{3+}In_{0.5}(PO_4)_3$	0.852 Mn^{2+}+0.148 In	0.826	2.22	0.75 Fe^{3+}+0.032 Mn^{2+}+0.218 In	0.685	2.09	[11]
$NaMnFe^{3+}In(PO_4)_3$	0.78 Mn^{2+}+0.22 In	0.823	2.22	0.5 Fe^{3+}+0.087 Mn^{2+}+0.413 In	0.724	2.10	[11]
$NaMnFe_{0.5}^{3+}In_{1.5}(PO_4)_3$	0.754 Mn^{2+}+0.246 In	0.823	2.23	0.64 In+0.25 Fe^{3+}+0.11 Mn^{2+}	0.765	2.12	[11]
$NaMnIn_2(PO_4)_3$	0.768 Mn^{2+}+0.232 In	0.823	2.23	0.85 In+0.15 Mn^{2+}	0.805	2.13	[11]
$Na_{1.5}Mn_{1.5}In_{1.5}(PO_4)_3$	0.928 Mn^{2+}+0.072 In	0.828	2.25	0.679 In+0.321 Mn^{2+}	0.810	2.14	[35]
$Na_2Mn_2Ga(PO_4)_3$	0.82 Mn^{2+}+0.18 Na	0.864	2.30	0.44 Mn^{2+}+0.5 Ga	0.675	2.05	[35]
$Na_2Mn_2Fe^{3+}(PO_4)_3$	0.88 Mn^{2+}+0.12 Na	0.853	2.24	0.5 Fe^{3+}+0.48 Mn^{2+}	0.721	2.10	[14]
$Na_2Mn_{1.5}Fe_{0.5}^{2+}Fe^{3+}(PO_4)_3$	0.95 Mn^{2+}+0.06 Na	0.841	2.19	0.5 Fe^{3+}+0.25 Fe^{2+}+0.21 Mn^{2+}	0.692	2.06	[14]
$Na_2MnFe^{2+}Fe^{3+}(PO_4)_3$	Mn^{2+}	0.830	2.18	0.5 Fe^{3+}+0.5 Fe^{2+}	0.713	2.07	[14]
$Na_2Mn_{0.5}Fe_{1.5}^{2+}Fe^{3+}(PO_4)_3$	0.5 Fe^{2+}+0.442 Mn^{2+}	0.757	2.20	0.5 Fe^{3+}+0.5 Fe^{2+}	0.713	2.05	[14]
$Na_2Fe_2^{2+}Fe^{3+}(PO_4)_3$	Fe^{2+}	0.780	2.19	0.5 Fe^{3+}+0.5 Fe^{2+}	0.713	2.06	[14]
$AgCaCdMg_2(PO_4)_3$	0.514 Ca+0.486 Cd	0.976	2.43	Mg	0.720	2.07	[17]
$AgCd_2Mg_2(PO_4)_3$	Cd	0.950	2.39	Mg	0.720	2.08	[17]
$Na_{1.50}Mn_{2.48}Al_{0.85}(PO_4)_3$	Mn^{2+}	0.830	2.248	0.573 Mn^{2+}+0.427 Al	0.704	2.067	[56]
$(Na,Ca)MnFe_2(PO_4)_3$	Mn^{2+}	0.830	2.223	0.645 Fe^{2+}+0.285 Fe^{3+}+0.045 Mn^{2+}+0.020 Mg	0.739	2.084	[6]
$(Na,Ca)MnFe_2(PO_4)_3$	Mn^{2+}	0.830	2.202	0.865 Fe^{3+}+0.105 Al+0.020 Mg+0.020 Mn^{2+}	0.645	2.034	[6]

cannot be introduced in significant amounts. These data have to be interpreted carefully, since Cu^{2+}, Ca^{2+}, Mg^{2+} and Ni^{2+} were successfully introduced in the alluaudite-type compounds $Cu_{1.35}Fe_3(PO_4)_3$ [38], $NaCaCdMg_2(PO_4)_3$ [30], and $Na_2(Mn_{1-x}M_x^{2+})Fe^{2+}Fe^{3+}(PO_4)_3$ ($M^{2+} = Mg^{2+}$, Ni^{2+}) [37], respectively.

When the substitution rate (x) in the $Na_{1.5}(Mn_{1-x}Zn_x^{2+})_{1.5}Fe_{1.5}(PO_4)_3$ solid solution increases, Zn^{2+}, which shows an effective ionic radius of 0.740 Å [34], is at first introduced in the $M(2)$ site, before to replace Mn^{2+} in the $M(1)$ site. The occupancy of $M(1)$ by small cations is not really surprising, since Mg^{2+} (effective ionic radius 0.720 Å [34]) has been introduced in this site in the compound $Na_2Mg_2Fe^{3+}(PO_4)_3$ [12]. The introduction of Zn^{2+} in alluaudite-type phosphates was not previously reported in the literature, but natural arsenates johillerite, $Na(Mg,Zn)_3Cu^{2+}(AsO_4)_3$, and o'danielite, $Na(Zn,Mg)_3H_2(AsO_4)_3$ [39], as well as the synthetic compound $AgZn_3H_2(AsO_4)_3$ [22], show significant amounts of this cation. Moreover, chemical analyses of natural alluaudites frequently contain small amounts of Zn^{2+}, which can reach 0.29 wt% ZnO [4,40–44].

The behavior of Cd^{2+} is very different from that of Zn^{2+}, since Cd^{2+} replaces first Mn^{2+} on the $M(1)$ site in the $Na_{1.5}(Mn_{1-x}Cd_x^{2+})_{1.5}Fe_{1.5}(PO_4)_3$ solid solution, before to occupy the $M(2)$ position. This behavior is due to the large effective ionic radius of Cd^{2+} (0.95 Å [34]), which explains its preference for the large

Table 10
Cation distributions in alluaudite-type phosphates.

Cation	*e.i.r.* (Å)		Site			
	[VI]	[VIII]	$A(2)'$	$A(1)$	$M(1)$	$M(2)$
Ag^+	1.15	1.28	X	X		
Na^+	1.02	1.18	X	X	X	
Cu^+	0.77	–	p	p		
Li^+	0.76	0.92	p	p		
Ca^{2+}	1.00	1.12	p	p	p	
Cd^{2+}	0.95	1.10		p	X	p
Mn^{2+}	0.830	0.96	p	p	X	X
Fe^{2+}	0.780	0.92			X	X
Co^{2+}	0.745	0.90			X	X
Zn^{2+}	0.740	0.90			X	p
Cu^{2+}	0.73	–		p		
Mg^{2+}	0.720	0.89			X	X
Ni^{2+}	0.690	–			X	X
In^{3+}	0.800	0.92			P	X
Fe^{3+}	0.645	0.78		p		X
Ga^{3+}	0.620	–				p
Cr^{3+}	0.615	–				p
Al^{3+}	0.535	–				p

X, complete occupancy of the site.p, Partial occupancy of the site.

$M(1)$ site. The incorporation of Cd^{2+} also induces a disordered cationic distribution of Cd^{2+} and Na^{+} on the $M(1)$ and $A(1)$ crystallographic sites; a disordered distribution which is similar to that previously observed in the $Na_2Cd_2M^{3+}(PO_4)_3$ ($M^{3+} = Fe^{3+}$, Ga^{3+}, Cr^{3+}) alluaudite-type compounds [12].

4.2. Cation distributions and variations of the M–O bond lengths in alluaudite-type phosphates

Site occupancies and average bond distances, available in the literature on alluaudite-type phosphates, are summarized in Table 9, and served us to draw Table 10. This last table shows that the $M(2)$ site of the alluaudite structure contains trivalents and divalent cations, with effective ionic radii between those of Al^{3+} (0.535 Å, [34]) and Cd^{2+} (0.95 Å, [34]). The $M(1)$ site accommodates mainly divalent cations, with effective ionic radii between those of Ni^{2+} (0.690 Å, [34]) and Ca^{2+} (1.00 Å, [34]), but can also contain significant amounts of In^{3+} (*e.i.r.*, 0.800 Å [34]) in the $NaMn(Fe_{1-x}In_x)_2(PO_4)_3$ and $Na_{1.5}Mn_{1.5}(Fe_{1-x}In_x)_{1.5}(PO_4)_3$ solid solutions [11,35], or be filled by Na^{+} (*e.i.r.* 1.02 Å, [34]) in $Na_3In_2(PO_4)_3$ [45].

The $A(2)'$ and $A(1)$ crystallographic sites, located in the channels of the alluaudite structure (Fig. 2), show similar crystal-chemical behaviors, with a strong affinity for the large monovalent cations Na^{+} (*e.i.r.* 1.18 Å, [34]) and Ag^{+} (*e.i.r.* 1.28 Å, [34]). However, these sites are able to accommodate much smaller cations, as for example Cu^{+} (*e.i.r.* 0.77 Å, [34]), Li^{+} (*e.i.r.* 0.92 Å, [34]), H^{+} (*e.i.r.* −0.38 Å, [34]) and Fe^{3+} (*e.i.r.* 0.78 Å, [34]). This observation demonstrates that the channels of the alluaudite structure, like the channels of minerals belonging to the beryl group or of cordierite [46–50], are able to contain cations with various effective ionic radii. When the channels contain large cations, such as Na^{+} or Ag^{+}, they are completely filled, while the smaller cations leave free space available. This feature explains why two H^{+} atoms are able to share the same channel in protonated alluaudite-type phosphates [26,27,29].

Finally, correlations were also established between the effective ionic radii of the cations occurring on the M sites and the M–O bond lengths (Figs. 15 and 16). These correlations are

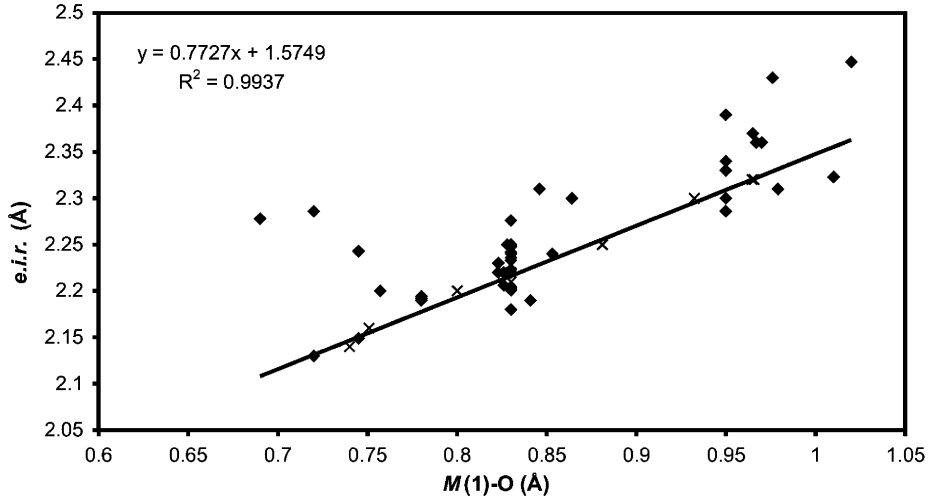

Fig. 15. Correlation between the $M(1)$–O distances and the ionic radii of the cations occurring in the $M(1)$ site, for alluaudite-type phosphates from the literature (dots) or investigated in the present study (crosses). The correlation line was calculated with the data from the present paper only.

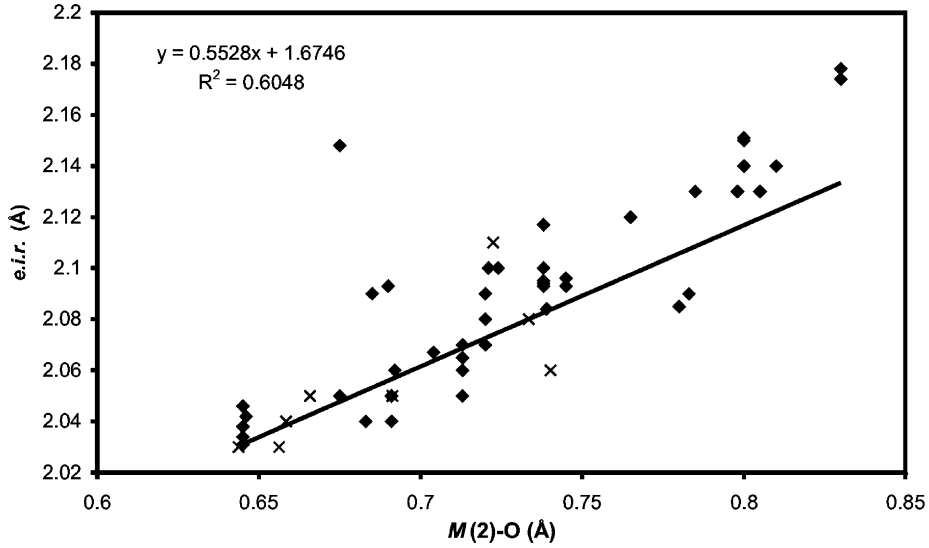

Fig. 16. Correlation between the $M(2)$–O distances and the ionic radii of the cations occurring in the $M(2)$ site, for alluaudite-type phosphates from the literature (dots) or investigated in the present study (crosses). The correlation line was calculated with the data from the present paper only.

generally satisfactory, except for a few data, which deviate from the general trends. These deviations are explained by the influence of the cations occurring in the neighboring *M* and *A* crystallographic sites [6].

Acknowledgments

The author is indebted to three anonymous reviewers as well as to A.-M. Fransolet, for his constructive comments and critical reading of the earlier versions of this manuscript. The "Fonds National de la Recherche Scientifique" (Belgium) is acknowledged for a position of "Chercheur Qualifié" and for the Grant 1.5.112.02. Many thanks to B. Belot who performed the wet chemical analyses.

References

[1] P. Černý, Geosci. Can. 18 (1991) 49–67.
[2] P.B. Moore, Am. Mineral. 56 (1971) 1955–1975.
[3] F. Hatert, P. Keller, F. Lissner, D. Antenucci, A.-M. Fransolet, Eur. J. Mineral. 12 (2000) 847–857.
[4] P.B. Moore, J. Ito, Mineral. Mag. 43 (1979) 227–235.
[5] F. Hatert, Mineral. Petrol. 81 (2004) 205–217.
[6] G. Redhammer, G. Tippelt, M. Bernroider, W. Lottermoser, G. Amthauer, G. Roth, Eur. J. Mineral. 17 (2005) 915–932.
[7] M. Auernhammer, H. Effenberger, G. Hentschel, T. Reinecke, E. Tillmanns, Mineral. Petrol. 48 (1993) 153–166.
[8] S.F. Solodovnikov, P.V. Klevstov, Z.A. Sodolovnikova, L.A. Glinskaya, R.F. Kletsova, J. Struct. Chem. 39 (1998) 230–237.
[9] G.D. Tsyrenova, S.F. Sodolovnikov, E.S. Zolotova, B.A. Tsybikova, Z.G. Bazarova, Russ. J. Inorg. Chem. 45 (2000) 103–108.
[10] F. Hatert, D. Antenucci, A.-M. Fransolet, M. Liégeois-Duyckaerts, J. Solid State Chem. 163 (2002) 194–201.
[11] F. Hatert, R.P. Hermann, G.J. Long, A.-M. Fransolet, F. Grandjean, Am. Mineral. 88 (2003) 211–222.
[12] D. Antenucci, Unpublished Ph.D. Thesis, University of Liège, 1992, 259 p.
[13] R.P. Hermann, F. Hatert, A.-M. Fransolet, G.J. Long, F. Grandjean, Solid State Sci. 4 (2002) 507–513.
[14] F. Hatert, L. Rebbouh, R.P. Hermann, A.-M. Fransolet, G.J. Long, F. Grandjean, Am. Mineral. 90 (2005) 653–662.
[15] F. Hatert, G.J. Long, D. Hautot, A.-M. Fransolet, J. Delwiche, M.-J. Hubin-Franskin, F. Grandjean, Phys. Chem. Miner. 31 (2004) 487–506.
[16] M.B. Korzenski, G.L. Schimek, J.W. Kolis, G.J. Long, J. Solid State Chem. 139 (1998) 142–160.
[17] M. Kacimi, M. Ziyad, F. Hatert, Mater. Res. Bull. 40 (2005) 682–693.
[18] T.E. Warner, W. Milius, J. Maier, Solid State Ion. 74 (1994) 119–123.
[19] A. Daidouh, C. Durio, C. Pico, M.L. Veiga, N. Chouaibi, A. Ouassini, Solid State Sci. 4 (2002) 541–548.
[20] C. Durio, A. Daidouh, N. Chouaibi, C. Pico, M.L. Veiga, J. Solid State Chem. 168 (2002) 208–216.
[21] T.J. Richardson, J. Power Sources 119–121 (2003) 262–265.
[22] P. Keller, H. Riffel, F. Zettler, H. Hess, Z. Anorg. Allg. Chem. 474 (1981) 123–134.
[23] H. Riffel, P. Keller, H. Hess, Z. Anorg. Allg. Chem. 530 (1985) 60–68.
[24] S. Khorari, Unpublished Ph.D. Thesis, University of Liège, 1997.
[25] N. Stock, G.D. Stucky, A.K. Cheetham, J. Phys. Chem. Solids 62 (2001) 1457–1467.
[26] F. Leroux, A. Mar, D. Guyomard, Y. Piffard, J. Solid State Chem. 117 (1995) 206–212.
[27] F. Leroux, A. Mar, C. Payen, D. Guyomard, A. Verbaere, Y. Piffard, J. Solid State Chem. 115 (1995) 240–246.
[28] A. Guesmi, A. Driss, Acta Crystallogr. C 58 (2002) i16–i17.
[29] K.-H. Lii, P.-F. Shih, Inorg. Chem. 33 (1994) 3028–3031.
[30] D. Antenucci, A.-M. Fransolet, G. Miehe, P. Tarte, Eur. J. Mineral. 7 (1995) 175–181.
[31] C.W. Burnham, LCLSQ version 8.4: Last-squares Refinement of Crystallographic Lattice Parameters, Department of Earth and Planetary Sciences, Harvard University, Cambridge, MA, 1991.
[32] R.A. Young, A.C. Larson, C.O. Paiva-Santos, User's Guide to Program DBWS-9807 for Rietveld Analysis of X-ray and Neutron Powder Diffraction Patterns, School of Physics, Georgia Institute of Technology, Atlanta, USA, 1998, 56 p.
[33] D. Antenucci, G. Miehe, P. Tarte, W.W. Schmahl, A.-M. Fransolet, Eur. J. Mineral. 5 (1993) 207–213.
[34] R.D. Shannon, Acta Crystallogr. A 32 (1976) 751–767.
[35] F. Hatert, Unpublished Ph.D. Thesis, University of Liège, 2002, 247 p.
[36] V.C. Farmer, The Infrared Spectra of Minerals, Mineralogical Society Monographs, London, 1974, 539 p.
[37] M. Rondeux, Unpublished Master Thesis, University of Liège, 2003, 51 p.
[38] T.E. Warner, W. Milius, J. Maier, Solid State Ion. 74 (1993) 119–123.
[39] P. Keller, H. Hess, N. Jb. Mineral. Mh. (1988) 395–404.
[40] P. Boury, Unpublished Master Thesis, University of Liège, 1981, 118 p.
[41] A.-M. Fransolet, P. Keller, F. Fontan, Contrib. Mineral. Petrol. 92 (1986) 502–517.
[42] P. Héreng, Unpublished Master Thesis, University of Liège, 1989, 101 p.
[43] E. Roda Robles, F. Fontan, A. Pesquera Pérez, P. Keller, Eur. J. Mineral. 10 (1998) 155–167.
[44] A.-M. Fransolet, F. Fontan, P. Keller, D. Antenucci, Can. Mineral. 36 (1998) 355–366.
[45] K.-H. Lii, J. Ye, J. Solid State Chem. 131 (1997) 131–137.
[46] D.L. Wood, K. Nassau, Am. Mineral. 53 (1968) 777–800.
[47] F.C. Hawthorne, P. Černý, Can. Mineral. 15 (1977) 414–421.
[48] J.P. Cohen, F.K. Ross, G.V. Gibbs, Am. Mineral. 62 (1977) 67–78.
[49] M.F. Hochella, G.E. Brown, F.K. Ross, G.V. Gibbs, Am. Mineral. 64 (1979) 337–351.
[50] J.H. Wallace, H.-R. Wenk, Am. Mineral. 65 (1980) 96–111.
[51] O.V. Yakubovich, M.A. Simonov, Y.K. Egorov-Tismenko, N.V. Belov, Sov. Phys. Dokl. 22 (1977) 550–552.
[52] N. Chouaibi, A. Daidouh, C. Pico, A. Santrich, M.L. Veiga, J. Solid State Chem. 159 (2001) 46–50.
[53] R. Ben Smail, T. Jouini, Acta Crystallogr. C 58 (2002) i61–i62.
[54] M. Hidouri, B. Lajmi, A. Driss, M. Ben Amara, Acta Crystallogr. E 59 (2003) i7–i9.
[55] M. Hidouri, B. Lajmi, A. Wattiaux, L. Fournés, J. Darriet, M.B. Amara, J. Solid State Chem. 177 (2004) 55–60.
[56] F. Hatert, Acta Crystallogr. C 62 (2006) i1–i2.